Optimum Spreading Bandwidth for DS-CDMA on Time and Frequency Fading Channels

by

Changqing Zheng

Submitted to the Department of Electrical Engineering and Computer Science
in partial fulfillment of the requirements for the degrees of

Bachelor of Science in Electrical Science and Engineering

and

Master of Engineering in Electrical Engineering and Computer Science

at the

MASSACHUSETTS INSTITUTE OF TECHNOLOGY

May 2002

Author .....
Department of Electrical Engineering and Computer Science
May 16, 2002

Certified by .....
Muriel Médard
Assistant Professor
Thesis Supervisor

Accepted by .....
Arthur C. Smith
Chairman, Department Committee on Graduate Students

Optimum Spreading Bandwidth for DS-CDMA on Time and Frequency Fading Channels

by

Changqing Zheng

Submitted to the Department of Electrical Engineering and Computer Science
on May 16, 2002, in partial fulfillment of the
requirements for the degrees of
Bachelor of Science in Electrical Science and Engineering
and
Master of Engineering in Electrical Engineering and Computer Science

Abstract

Spread spectrum communication systems have seen widespread usage in wireless systems. Spreading is used to provide diversity in frequency and results in a number of benefits. However, recent literature has shown that for a channel that decorrelates in time and frequency, and given second and fourth moment constraints that decay inversely and inverse squared, respectively, with the spreading bandwidth, the capacity of a wideband system in a fading channel goes to zero in the limit of infinite bandwidth. Despite the detrimental asymptotic performance of wideband systems, there may still be an appropriate range within which spread spectrum techniques can be gainfully employed. By adapting the upper bound from Médard and Tse [12], and deriving a suitable lower bound, it is possible to obtain the desired range for the optimal spreading bandwidth. The single user result is then extended to the two user case as a representative example of the multiple access scenario. For both the single user case and the two user case, this thesis shows that there exist a non-trivial minimum spreading bandwidth that correlates closely with those parameters used by commercial spread spectrum systems. Furthermore, given typical system and channel parameters, the minimum spreading bandwidth behaves as a linear function of the energy of the propagation coefficient.

Thesis Supervisor: Muriel Médard
Title: Assistant Professor

Acknowledgments

I wish to thank my thesis supervisor, Professor Muriel Médard, for her patience and guidance throughout this thesis and my graduate education at MIT.

I wish to thank my parents and my brother for their love and encouragement throughout my years of growing up, and especially during this stressful year of thesis undertaking.

I would also like to thank Mingxi Fan for his help throughout my undergraduate and graduate education at MIT. The many hours of discussions gave me a greater understanding of the exciting field of wireless communications.

Lastly, I wish to thank all my friends at MIT for making the past five years fun and memorable.

Contents

List of Figures

List of Tables

Chapter 1

Introduction

In spread spectrum communication systems, a signal is made to occupy a bandwidth beyond that which is minimally required prior to being transmitted. This bandwidth expansion factor is referred to as the processing gain. Spreading of a signal is generally obtained through direct sequence or frequency hopping techniques. In frequency hopping techniques, in a pseudorandom manner, the signal is made to occupy different frequency bands at different times so that the effective bandwidth occupied by the signal over time is much greater. If the hopping pattern for each user is constructed such that only one user occupies a particular section of the bandwidth at a time, then frequency hopping spread spectrum reduces to a frequency division multiple access (FDMA) problem with added diversity.

By contrast, in direct sequence spread spectrum, also call direct sequence code division multiple access (DS-CDMA), each user is assigned a code and shares the bandwidth with all other users. Each bit of the original signal is multiplied by the spreading code to create a string of "chips" to achieve the desired enlargement of occupied bandwidth. At the receiver, synchronized reception using the spreading code performs the despreading and the subsequent data recovery. Under certain channel conditions, if orthogonal codes are used, the users will not interfere with each other. Otherwise, codes with low cross-correlation, such as Gold codes in the uplink of Wideband-CDMA, are used to mitigate the effect of multiple access interference.

At the cost of extra bandwidth, spreading produces a number of benefits, of

which the military was the first to exploit. Spread spectrum techniques produce anti-jamming and low detectability properties that have been of particular interest to the military. The wideband property of a spread spectrum signal reduces the effectiveness of a hostile jammer by forcing it to distribute its finite resources (power) over a wider bandwidth. Furthermore, in direct sequence spread spectrum, because of the processing gain at the receiver, a signal can be transmitted well below the ambient noise level, rendering detection by hostile parties difficult. At the same time, after despreading, the processing gain allows the signal to still be received with sufficient Signal to Noise Ratio (SNR) for proper decoding. Therefore, everything else being equal, a spread spectrum signal is more likely to be received accurately through a jamming environment.

As cellular wireless communication began to be widely used, researchers began to investigate spread spectrum techniques for multiple access purposes. Spread spectrum multiple access techniques, more specifically Direct Sequence Code Division Multiple Access (DS-CDMA) offers a number of advantages over Frequency Division Multiple Access (FDMA) and Time Division Multiple Access (TDMA), the competing forms of multiple access techniques. The DS-CDMA variant of spread spectrum promises two important benefits over TDMA and FDMA: optimal frequency reuse, soft user-capacity constraint and graceful degradation of performance. Partly due to these benefits, the DS-CDMA variant of spread spectrum has gained widespread acceptance as the technology of choice for the Third Generation cellular mobile communication systems.

1.1 Motivations

Spread spectrum systems first saw use in the 1970's when the military made use of its anti-jamming and low detectability properties. In the 1990's, Qualcomm pioneered the commercial application of CDMA systems, first in Omnitrac, a tracking system for trucks, and then in IS-95 CDMA, a cellular mobile radio system. At present, all Third Generation cellular mobile communication systems (W-CDMA, CDMA2000) that

are deployed or slated for deployment are based on DS-CDMA principles. However, until recently, little has been done to study the effect of spreading bandwidth on the capacity of communications systems operating in a wireless environments.

The wide use of DS-CDMA systems entails that the study of the capacity regions of spread spectrum systems in wireless environments is highly relevant to effective deployment of new systems. When a CDMA system using white-noise like signals is spread to increasingly large bandwidths, it becomes increasingly difficult for the rake receiver to measure the channel and correspondingly more difficult for detection to take place. Determining the capacity regions of a spread spectrum system makes it possible to determine the range of bandwidths to which a signal should be spread. The outcome of this thesis will hopefully aid future wireless system engineers to optimize bandwidth usage given design parameters.

1.2 Existing Results

The information theoretic study of wideband fading channels dates back to the 1960's when Kennedy in [7] showed that the capacity of an infinite bandwidth Rayleigh fading channel is equal to that of an infinite bandwidth additive white Gaussian noise (AWGN) channel. In the last decade or so, further research into wideband fading channels has yielded a wealth of significant new results. Recent results in the professional literature on this topic relate to the capacity of a wideband channel as the spreading bandwidth is increased to infinity.

In [11], Médard considered bandwidth scaled spreading over independent fading channels. The available bandwidth is divided into contiguous slices of equal size, and the available power is distributed evenly over the entire spectrum. Within each bandwidth slice the signaling method is unchanged except for the downward scaling in power as the total bandwidth is increased. Using this model, the author showed that for large bandwidth DS-CDMA, spreading has adverse effects on the achievable rate when the channel truly decorrelates in frequency or when the channel bandwidth slices are correlated but not jointly estimated.

In [13], Médard and Gallager further extended the result in [11] to show that very large bandwidths cannot be effectively utilized by spread spectrum systems that spread the available power uniformly over both time and frequency. By expressing the input process as an expansion localized in time and frequency of orthonormal set of functions, the fourth moment of each coefficient of this expansion is uniformly constrained. Such a uniform constraint of the fourth moment forces the mutual information to decay to zero inversely with increasing bandwidth. This result suggest that conventional DS-CDMA systems do not scale well to extremely large bandwidths. Therefore, ultra wideband systems using uniform signaling over time and frequency over gigahertz of bandwidth should only be used over quasi-static channels [13].

Related to the result of [13] are those of Subramanian and Hajek, where the authors showed an alternate derivation using using the theory of capacity per unit cost for fourthegy. The results in [14] reinforces the conclusion in [13] that signals need to be bursty in time and/or frequency to be able to achieve constant mutual information rates per unit power over ultra-wideband wide-sense-stationary uncorrelated scattering fading channels [14]. Another recent result by Hajek and Subramanian is one that considered a peak signal constraint going to zero [6]. The authors showed the difficulty of transmitting small peak constrained signals over Rayleigh fading channels.

Other related results include [15], where the authors consider a wideband multipath fading channel and showed that, subject to energy constraint, the capacity of the channel is inversely proportional to the number of resolvable paths. While in this case bandwidth does not directly affect capacity, if the number of paths is very large and the delays between paths are significant, then the number of resolvable paths increases with bandwidth. As the number of resolvable paths increase, capacity suffers. Furthermore, the above result holds even if the receiver is able to perfectly track the timing of the different paths. If the receiver does not have perfect timing knowledge, then the capacity of the channel goes to zero as bandwidth increases to infinity irrespective of the number of resolvable paths.

All of the results above consider the upper limit to capacity and does not offer a range for the optimal spreading bandwidth. Despite the detrimental asymptotic

performance of wideband systems, there must still be an appropriate range within which spread spectrum techniques can be gainfully employed. By combining an upper bound with a suitable lower bound, it is possible to obtain the desired range for the optimal spreading bandwidth.

1.3 Thesis Outline

The scope of this thesis will cover both the single user scenario as well as the two user scenario as a representative example of the multi-user case for a channel that decorrelates in time and frequency, and using DS-CDMA signaling. In the single user case, a theoretical analysis will be performed and insights distilled from the results. These will then be expanded to the two-user scenario. Below is a chapter by chapter breakdown of the contents.

Chapter Two describes the channel model, and the theoretical analysis leading to the upper and lower capacity bounds in the single user scenario. Derivation of the upper and lower bounds to capacity is followed by analysis of various ranges of parameters and the resulting optimum spreading bandwidth.

Chapter Three describes the channel model, and the theoretical analysis leading to the upper and lower capacity bounds in the two-user multiple access scenario. Derivation of the upper and lower bounds to capacity are followed by analysis of the capacity bounds in the two-user multiple access scenario for various ranges of parameters and the resulting optimum spreading bandwidth.

Chapter Four will summarize the results of the thesis and point to possible areas for future work.

Chapter 2

Analysis of Single User Scenario

In this chapter a time and frequency block fading channel model is developed. Using this model, an upper bound, along with an appropriate lower bound is derived. In mobile communications, the transmitted signals are subject to additional disruptive environmental factors not present in traditional wire-line communications. These disruptive factors cannot be controlled or predicted, and can at best be modeled as stochastic processes and analyzed as such. In mobile communications in a wireless environment, the receiver must contend with a multiplicative noise, as well as the additive receiver noise, that further degrades the transmitted signal. Fading is the term given to this multiplicative noise in the aggregate and is in part the result of time varying multipath. In fact, multipath accounts for most deep fades and may change far more rapidly than other fading phenomenon, such as scattering.

Multipath results from the signal reflecting upon obstacles and arriving at the receiver with different time delays. Absent additive noise, in a stationary, non-changing environment, multipath as a linear, time-invariant (LTI) phenomenon can be effectively combatted using standard LTI filtering techniques such as echo cancellation filters. However, multipath is entirely dependent on the transmission environment, and in mobile communications, the mobile nature of the transmitter and receiver produces added challenges. Owing to the constantly changing surroundings of the transmitter and receiver, multipath in mobile communications is a time-varying process and traditional LTI techniques no longer apply.

Associated with multipath in mobile communications is the Doppler effect. The Doppler effect encompass two related phenomenon, the Doppler shift and the Doppler spread. Suppose the sender transmits a sinusoid of frequency f_0, then the receiver receives a sinusoid of frequency f_R. The difference between f_0 and f_R is the Doppler shift and results from the relative motion between the transmitter and receiver. Relative to the sender, if the receiver is moving away from the sender, then $f_0 > f_R$. Conversely, if the receiver is moving towards the sender, then $f_0 < f_R$. The magnitude of the Doppler shift B is a function of the relative velocity $\overline{\omega}$ and the sender carrier frequency f_0 given by the following:

$$B = f_0 \frac{\overline{\omega}}{c} \tag{2.1}$$

where c is the speed of light. A derivation of Equation 2.1 can be found in [10], pp. 22-23.

Without multipath, the Doppler shift can be compensated at the receiver by adjusting the frequency oscillator. With the additional effect of multipath, each path arriving at the receiver experiences its own frequency shift. Like multipath, the Doppler shifts in mobile communication are also time-varying. Additionally, the range of Doppler shifts experienced by the different paths together constitute the Doppler spread that enlarges the bandwidth occupied by the signal. Generally however, the bandwidth expansion contributed by the Doppler spread is small compared to the channel spacing usually considered, and its effect can be considered negligible. While the bandwidth expansion effect can in general be neglected, the time varying characteristic of the Doppler shift represent the speed at which the phase changes.

2.1 Channel Model

This section presents a simplified block fading model that captures the decorrelation in time and frequency. Decorrelation in time and frequency are the important characteristics that motivate the use of the block fading model. With decorrelation in time, the

Parameter	Description	Constraints/Distribution
W	coherence bandwidth size	
μ	number of coherence bands	$\mu \in \{\text{positive integers}\}$
$\mathcal{E}$	total average power	
T	length of coherence time	
γ	peakiness of the signal	
$F[i]$	propagation coefficient in coherence band i	$F[i]$ is zero mean, circularly symmetric, complex Gaussian. $E[F^2] = \sigma_F^2$
$X[i]_j$	input at sample time j in coherence band i	$E[X^2] \leq \frac{\mathcal{E}}{\mu}$ $\lvert X \rvert \leq \frac{\gamma}{\mathcal{E}}\sqrt{E[X^2]} = \frac{\gamma}{\sqrt{\mathcal{E}\mu}}$
$Z[i]_j$	noise at sample time j in coherence band i	$Z[i]_j$ is zero mean, circularly symmetric, complex with normalized unit variance

Table 2.1: Summary of Channel Model Parameters

fading coefficient between coherence time intervals are uncorrelated. This is critically related to the length of each coherence time interval. If the coherence time is large, then decorrelation in time is unlikely. With coherence time $T \propto \frac{1}{\text{Doppler spread}}$, and Doppler spread on the order of 10 Hz to 100 Hz, that gives a coherence time on the order of 0.01 sec to 0.1 sec. With decorrelation in frequency, the fading coefficient between different coherence bands are uncorrelated. This is critically related to the size of the coherence bandwidth. If the coherence bandwidth is large, then decorrelation in frequency is unlikely. With coherence bandwidth $W \propto \frac{1}{\text{delay spread}}$, and delay spread typically on the order of microseconds (μs) to tens of microseconds, that gives a coherence bandwidths on the order of 100 KHz to 1 MHz. Therefore, as long as T and W remain within these typical bounds, decorrelation in time and frequency can be assumed to be valid. So long as W remains inside the typical bounds of coherence bandwidth, all frequency components undergo the same attenuation and phase change. Moreover, if the channel decorrelates in time (i.e., multipath components are separated by less than the coherence time), then the different paths cannot be resolved and flat fading can be assumed. For a channel that decorrelates in time and frequency, it can be modeled as Rayleigh flat fading.

The channel model used for this single user scenario is based on that described

in [9], and extended in [12]. This is a standard Rayleigh flat fading channel that undergoes block fading in time and frequency. Each channel over distinct coherence bandwidths are independent, and transmission occurs over μ distinct coherence bandwidths. The propagation coefficient for each coherence bandwidth remains constant for T, the coherence time, after which it changes to a new independent value. These random propagation coefficients are modeled as independent, identically distributed, zero mean, complex circularly symmetric Gaussian random variables. In addition to the multiplicative noise associated with Rayleigh fading, there is also the standard additive receiver noise. Here, the additive noise is also modeled as a zero mean, complex circularly symmetric Gaussian random variable, normalized to unit variance.

Each coherence band is of size W, and samples are obtained at the Nyquist rate of W samples per second. Thus within the coherence time T there are a total of TW samples and the received vector in the i^{th} coherence band over the j^{th} coherence time is:

$$Y[i]_{jTW+1}^{(j+1)TW} = F[i]_j X[i]_{jTW+1}^{(j+1)TW} + Z[i]_{jTW+1}^{(j+1)TW} \tag{2.2}$$

Naturally there is an average power constraint imposed on the $X[i]_j's$, for without an average power constraint then the channel can achieve an arbitrarily large data rate. Thus a limited amount of power $\mathcal{E}$ is distributed equally to each of the μ coherence bands, yielding an upper bound on the second moment given by $E\left[X[i]_j^2\right] \leq \frac{\mathcal{E}}{\mu}$. Additionally, in practical communication systems, there may be peak power constraints, leading to an upper bound on the peak amplitude. The peak amplitude is upper bounded by $|X| \leq \frac{\gamma}{\mathcal{E}}\sqrt{E\left[X[i]_j^2\right]}$, where γ is defined as the peakiness of the signal. Table 2.1 summarizes the parameters of the channel model.

2.1.1 Brief Note on Notation

The following notation is used throughout the thesis: $\log x$ is the base-two logarithm of x, while $\ln x$ is base e logarithm.

2.2 Upper Bound to Wideband Capacity

Based on the channel model, within each coherence band there is an average power constraint corresponding to an upper bound on the second moment of the signal. However, only signals which satisfy the second moment constraint with equality can achieve the upper bound to capacity. Suppose that an upper bound is derived using signals which do not satisfy the second moment constraint with equality, then by the data processing inequality, the capacity of the channel with the input multiplied by some constant α would be greater than that of the channel not multiplied by α. Keeping that in mind, Lemma 1 gives the upper bound to capacity in the single user scenario, which follows from the derivation in [12].

Lemma 1 *The upper bound on wideband capacity based on the channel model described in Section 2.1 is:*

$$C\left(W, \mathcal{E}, \sigma_F^2, T, \mu, \gamma\right) \leq W\mu \log\left(\sigma_F^2 \frac{\mathcal{E}}{\mu} + 1\right) - \frac{\mathcal{E}^2 \mu}{\gamma^2 T} \log\left(TW \frac{\gamma^2}{\mu \mathcal{E}} \sigma_F^2 + 1\right) \tag{2.3}$$

Proof:

$$C = \lim_{k \to \infty} \max_{p_X} \left(\frac{1}{k} \sum_{j=1}^{k} \sum_{i=1}^{\mu} \frac{1}{T} I(\underline{X}[i]_{jTW+1}^{(j+1)TW}; \underline{Y}[i]_{jTW+1}^{(j+1)TW}) \right) \tag{2.4}$$

The fourth central moment of $X[i]_j$ is $\frac{\gamma}{\mu^2}$ and its average power constraint is $\frac{\mathcal{E}}{\mu}$. Since there are no sender channel side information and all the bandwidth slices are independent, applying the concavity of mutual information in the input distribution results in selecting all the inputs to be IID to maximize the righthand side (RHS) of Equation 2.4.

First rewrite mutual information in terms of entropy:

$$\begin{aligned} & \frac{1}{T} I(\underline{X}[i]_{jTW+1}^{(j+1)TW}; \underline{Y}[i]_{jTW+1}^{(j+1)TW}) \\ = \; & \frac{1}{T} h(\underline{Y}[i]_{jTW+1}^{(j+1)TW}) - \frac{1}{T} h(\underline{Y}[i]_{jTW+1}^{(j+1)TW} \mid \underline{X}[i]_{jTW+1}^{(j+1)TW}) \end{aligned} \tag{2.5}$$

Now find a suitable upper bound to Equation 2.5. First upper bound $h(\underline{Y})$

$$\begin{aligned}
\frac{1}{T}h(\underline{Y}[i]_{jTW+1}^{(j+1)TW}) &\overset{a}{\leq} \frac{1}{T}\log\left((\pi e)^{TW}|\Lambda_{\underline{Y}[i]_{jTW+1}^{(j+1)TW}}|\right) \qquad (2.6)\\
&\overset{b}{\leq} \frac{1}{T}\log\left((\pi e)^{TW}\prod_{m=1}^{TW}(\sigma_F^2\sigma_{X_m}^2+1)\right)\\
&= W\log(\pi e)+\frac{1}{T}\sum_{m=1}^{TW}\log\left(\sigma_F^2\sigma_{X_m}^2+1\right)\\
&\overset{c}{\leq} W\log(\pi e)+W\log\left(\sigma_F^2\frac{\mathcal{E}}{\mu}+1\right) \qquad (2.7)
\end{aligned}$$

(a) follows because entropy is maximized by a Gaussian distribution for a given covariance matrix. Equation 2.6, which gives the entropy of a zero mean, complex circularly symmetric Gaussian random vector, follows from Lemma 6 given in Appendix A.

(b) follows from Hadamard's inequality [3].

(c) follows from the average power constraint of the channel model.

Next find a suitable lower bound to $h(\underline{Y}|\underline{X})$

$$\begin{aligned}
\frac{1}{T}h(\underline{Y}[i]_{jTW+1}^{(j+1)TW} \mid \underline{X}[i]_{jTW+1}^{(j+1)TW}) &\overset{a}{=} \frac{1}{T}E_X\left[\log\left((\pi e)^{TW}|\Lambda_{\underline{Y}[i]_{jTW+1}^{(j+1)TW}|\underline{X}[i]_{jTW+1}^{(j+1)TW}}|\right)\right]\\
&\overset{b}{=} \frac{1}{T}E_X\left[\log\left((\pi e)^{TW}(\sigma_F^2\|\underline{X}\|^2+1)\right)\right]\\
&= W\log(\pi e)+\frac{1}{T}E_X\left[\log(\sigma_F^2\|\underline{X}\|^2+1)\right] \qquad (2.8)
\end{aligned}$$

(a) results from the fact that conditioned on $\underline{X}[i]_{jTW+1}^{(j+1)TW}$, $\underline{Y}[i]_{jTW+1}^{(j+1)TW}$ is a zero mean, complex circularly symmetric Gaussian random vector.

(b) follows from taking the determinant of the conditional covariance matrix, which

is given by the following:

$$\Lambda_{\underline{Y}|\underline{X}} = \begin{bmatrix} \sigma_F^2 x[1]^2 + 1 & \sigma_F^2 x[1]x[2] & \cdots & \sigma_F^2 x[1]x[TW] \\ \sigma_F^2 x[2]x[1] & \sigma_F^2 x[2]^2 + 1 & \cdots & \sigma_F^2 x[2]x[TW] \\ \vdots & \vdots & \ddots & \vdots \\ \sigma_F^2 x[TW]x[1] & \sigma_F^2 x[TW]x[2] & \cdots & \sigma_F^2 x[TW]^2 + 1 \end{bmatrix}$$

the eigenvalues of $\Lambda_{\underline{Y}[i]_{jTW+1}^{(j+1)TW}|\underline{X}[i]_{jTW+1}^{(j+1)TW}}$ follows from Lemma 7 given in Appendix A, and taking the product of the eigenvalues gives the resulting determinant.

Any particular signaling scheme would constitute a valid lower bound to capacity so long as it satisfied the conditions outlined in the channel model. Therefore, a suitable lower bound to Equation 2.8 can be obtained by using a binary signal constellation that satisfies the second moment constraint and the peak amplitude constraint with equality. X is therefore distributed as follows:

$$X = \begin{cases} 0 & \text{with prob. } 1 - \frac{\mathcal{E}^2}{\gamma^2} \\ \frac{\gamma}{\sqrt{\mu\mathcal{E}}} & \text{with prob. } \frac{\mathcal{E}^2}{\gamma^2} \end{cases}$$

thus, using this distribution and applying the concavity of the log function, Equation 2.8 can be lower bounded as:

$$\frac{1}{T} h(\underline{Y}[i]_{jTW+1}^{(j+1)TW} \mid \underline{X}[i]_{jTW+1}^{(j+1)TW}) \geq W \log(\pi e) + \frac{\mathcal{E}^2}{T\gamma^2} \log\left(TW \frac{\gamma^2}{\mu\mathcal{E}} \sigma_F^2 + 1\right) \qquad (2.9)$$

Substituting Equations 2.7 and 2.9 into Equation 2.5 and taking the limit in Equation 2.4 yields the desired result. ***Q.E.D.***

2.2.1 Tightness of the Upper Bound

Based on research work already published in the literature on the capacity of wideband fading channels, it is expected that a suitable upper bound to capacity for this channel model would also behave similarly. Specifically, in the limit of infinite bandwidth, capacity should converge to zero from above. Therefore, having derived an upper

bound in Lemma 1, it is now necessary to make sure that Equation 2.3 does indeed converge to zero as $\mu \to \infty$.

$$\begin{aligned}
& \lim_{\mu\to\infty} W\mu \log\left(\sigma_F^2 \frac{\mathcal{E}}{\mu} + 1\right) - \frac{\mathcal{E}^2\mu}{\gamma^2 T} \log\left(TW\frac{\gamma^2}{\mu\mathcal{E}}\sigma_F^2 + 1\right) \\
& \text{setting } x = \tfrac{1}{\mu} \text{ and applying L'Hospital's rule:} \\
= & \lim_{x\to 0^+} \frac{W}{x} \log\left(\sigma_F^2\mathcal{E}x + 1\right) - \frac{\mathcal{E}^2}{\gamma^2 T x} \log\left(TW\frac{\gamma^2 x}{\mathcal{E}}\sigma_F^2 + 1\right) \\
= & \lim_{x\to 0^+} \frac{W\sigma_F^2\mathcal{E}}{\sigma_F^2\mathcal{E}x + 1} - \frac{W\sigma_F^2\mathcal{E}}{TW\frac{\gamma^2\sigma_F^2}{\mathcal{E}}x + 1} \\
= & \; W\sigma_F^2\mathcal{E} - W\sigma_F^2\mathcal{E} \\
= & \; 0
\end{aligned}$$

Therefore, the above derivation shows that Equation 2.3 does indeed provide a sufficiently tight upper bound to the wideband capacity.

2.3 Lower Bound to Wideband Capacity

There are many different possible lower bounds to capacity. One approach would be to start from the definition of mutual information as in the upper bound, and apply information theory inequalities to obtain a lower bound. Another approach is to devise a particular signaling scheme, and either compute the exact achievable rate or obtain a lower bound. Either method produces a valid lower bound. In this case, the second approach is favored because a signaling scheme can be chosen whose achievable rate can be easily determined.

2.3.1 A Binary Signaling Scheme

In [1] the authors determined that for a power constrained discrete-time Rayleigh fading channel, in which successive symbols face independent fading and neither sender nor receiver has channel state information, the capacity achieving a distribution is discrete with a finite number of mass points. One of the mass points of this discrete finite mass point distribution is located at the origin. Additionally, for low signal

to noise ratio, a binary signal gives relatively good performance. Therefore, a simple signaling scheme is one where the transmitter sends binary signals, one of which is located at the origin. As in the upper bound, let the $X[i]'_j s$ be chosen IID, and $X[i]_j \in \{0, \alpha\}$ with the following distribution:

$$X = \begin{cases} 0 & \text{with prob. } 1-p \\ \alpha = \sqrt{\frac{\mathcal{E}}{\mu p}} \leq \frac{\gamma}{\sqrt{\mu \mathcal{E}}} & \text{with prob. } p \end{cases} \tag{2.10}$$

The above distribution satisfies the second moment constraint with equality, and keeping the peak amplitude constraint in mind, the peakiness $\gamma \geq \frac{\mathcal{E}}{\sqrt{p}}$. Because γ does not directly factor into the second moment constraint, varying γ in this distribution gives one extra degree of freedom in adjusting the resulting capacity. Once transmitted, the receiver performs Maximum a Posteriori Probability (MAP) detection to recover the transmitted signal. Having constructed the signaling scheme, Lemma 2 gives the lower bound to capacity

Lemma 2 *The lower bound to wideband capacity based on the channel model described in Section 2.1 and the particular signaling scheme with MAP detection given in Section 2.3.1 is:*

$$\begin{aligned} C\left(W, \mathcal{E}, \sigma_F^2, T, \mu, \gamma, p\right) \geq\ & W\mu \left[(1-r)\log\frac{1}{1-r} + r\log\frac{1}{r}\right] \\ & - W\mu\,(1-p)\,\left[(1-p_0)\log\frac{1}{1-p_0} + p_0\log\frac{1}{p_0}\right] \\ & - W\mu\,p\,\left[(1-p_\alpha)\log\frac{1}{1-p_\alpha} + p_\alpha\log\frac{1}{p_\alpha}\right] \end{aligned} \tag{2.11}$$

where

$$\begin{aligned} p_0 &= \exp\left(-\beta^2\right) \\ p_\alpha &= 1 - \exp\left(-\frac{\beta^2}{\sigma_1^2}\right) \\ r &= (1-p)\exp\left(-\beta^2\right) + p\exp\left(-\frac{\beta^2}{\sigma_1^2}\right) \\ \beta^2 &= \frac{\sigma_1^2}{\sigma_1^2 - 1}\ln\left[\frac{(1-p)\sigma_1^2}{p}\right] \end{aligned}$$

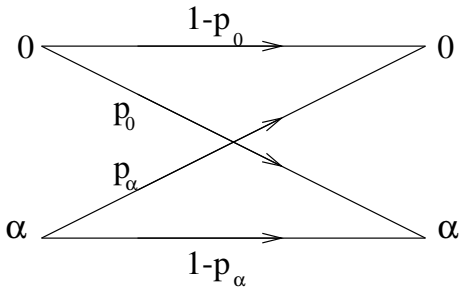

Figure 2-1: Discrete Binary Channel with cross-over probabilities p_0 and p_α

$$\sigma_1^2 = \frac{\mathcal{E}}{\mu p}\sigma_F^2 + 1$$

Proof:

During transmission through the communication channel the signal is corrupted by multiplicative and additive noise. Applying MAP detection reduces the channel into a discrete binary channel with cross-over probabilities p_0 and p_α, as shown in Figure 2-1.

To calculate the cross-over probabilities, the detection threshold must first be calculated:

- let $CN(0, \sigma^2)$ represent the PDF of a zero mean, complex circularly symmetric Gaussian random variable with variance σ^2.

$$f_X(x) = CN(0, \sigma^2) = \frac{1}{\pi\sigma^2}\exp\left(-\frac{|x|^2}{\sigma^2}\right)$$

- given a "0" is send, the distribution of the received signal is $f_{Y|X}(y|x = 0) = CN(0, 1)$; given an "$\alpha$" is send, the distribution of the received signal is $f_{Y|X}(y|x = \alpha) = CN(0, \alpha^2\sigma^2 + 1)$.

- for the complex received signal, the detection threshold is determined wholly by its magnitude, and can be found by solving the following equation:

$$(1 - p) f_{Y|X}(y|x = 0) = (p) f_{Y|X}(y|x = \alpha)$$

$$
\begin{aligned}
(1-p)CN(0,1) &= (p)CN(0,\alpha^2\sigma_F^2+1) \\
\text{letting } \sigma_1^2 &= \alpha^2\sigma_F^2+1 \\
(1-p)\frac{1}{\pi}\exp\left(-|y|^2\right) &= (p)\frac{1}{\pi\sigma_1^2}\exp\left(-\frac{|y|^2}{\sigma_1^2}\right) \\
\text{solving the above equation} & \\
|y| &= \sqrt{\frac{\sigma_1^2}{\sigma_1^2-1}\ln\left[\frac{(1-p)\sigma_1^2}{p}\right]} \qquad (2.12)
\end{aligned}
$$

- the detection threshold based solely on the **magnitude** of the received complex signal is that given in Equation 2.12.

Having determined the detection threshold as given in Equation 2.12, the crossover probabilities can be calculated by integrating over the corresponding decision regions. Since only the magnitude factors into the decision regions, the conditional PDF of the **magnitude** ϱ of the received signal, by a simple change of variable plus accounting for the phase, is Rayleigh distributed given by the following:

$$
\begin{aligned}
f_{\varrho|X}(\varrho|x=0) &= (2\varrho)\exp\left(-\varrho^2\right) \quad \text{for } \varrho \geq 0 \\
f_{\varrho|X}(\varrho|x=\alpha) &= \left(\tfrac{2\varrho}{\sigma_1^2}\right)\exp\left(-\tfrac{\varrho^2}{\sigma_1^2}\right) \quad \text{for } \varrho \geq 0
\end{aligned}
$$

Let β be the detection threshold given by Equation 2.12, the crossover probabilities p_0 and p_α are:

$$
\begin{aligned}
\beta^2 &= \frac{\sigma_1^2}{\sigma_1^2-1}\ln\left[\frac{(1-p)\sigma_1^2}{p}\right] \\
p_0 &= \int_\beta^\infty f_{\varrho|X}(\varrho|x=0)\,d\varrho \\
&= \exp\left(-\beta^2\right) \qquad (2.13) \\
p_\alpha &= \int_0^\beta f_{\varrho|X}(\varrho|x=\alpha)\,d\varrho \\
&= 1-\exp\left(-\frac{\beta^2}{\sigma_1^2}\right) \qquad (2.14)
\end{aligned}
$$

Given the crossover probabilities, the probability r of receiving an α can be easily

calculated:

$$
\begin{aligned}
r = p_Y(y=\alpha) &= (1-p)p_0 + (1-p_\alpha)p \qquad (2.15)\\
&\text{substituting in Equations 2.13 and 2.14}\\
r &= (1-p)\exp\left(-\beta^2\right) + p\exp\left(-\frac{\beta^2}{\sigma_1^2}\right)
\end{aligned}
$$

The mutual information of a single use of the discrete binary channel is given by:

$$
\begin{aligned}
I(Y;X) &= H(Y) - H(Y|X)\\
&\text{for a discrete binary distribution}\\
&\text{with probabilities } a \text{ and } 1-a, \text{ let}\\
H(a) &= a\log\frac{1}{a} + (1-a)\log\frac{1}{1-a}\\
&\text{therefore, for a single use of the channel}\\
I(Y;X) &= H(r) - E_x\left[H(Y|X=x)\right]\\
&= H(r) - pH(p_\alpha) - (1-p)H(p_0) \qquad (2.16)
\end{aligned}
$$

Substituting r, p_0, p_α from Equations 2.15, 2.13, and 2.14, respectively, into Equation 2.16, and multiplying by $W\mu$ to account for the $W\mu$ uses of the channel per second yields the capacity in bits/second as given in Equation 2.11. ***Q.E.D.***

2.3.2 Tightness of the Lower Bound

Having established that the upper bound given by Equation 2.3 of Lemma 1 is asymptotically tight, it stands to reason that the lower bound must also be asymptotically tight as well. The lower bound given by Equation 2.11 of Lemma 2 is mainly a function of the crossover probabilities p_0 and p_α. The crossover probabilities are functions of β^2, which is a function of σ_1^2, which is a function of μ. Taking their limits as $\mu \to \infty$:

$$
\lim_{\mu\to\infty}\sigma_1^2 = \lim_{\mu\to\infty}\frac{\mathcal{E}}{\mu p}\sigma_F^2 + 1
$$

$$
\begin{aligned}
&= 1 \\
\lim_{\mu\to\infty} p_0 &= \lim_{\mu\to\infty} \exp\left(-\beta^2\right) \\
&= \lim_{\mu\to\infty} \exp\left(-\frac{\sigma_1^2}{\sigma_1^2-1}\ln\left[\frac{(1-p)\sigma_1^2}{p}\right]\right) \\
&= \lim_{\sigma_1^2\to 1} \exp\left(-\frac{\sigma_1^2}{\sigma_1^2-1}\ln\left[\frac{(1-p)\sigma_1^2}{p}\right]\right) \\
&= 0 \\
\lim_{\mu\to\infty} p_\alpha &= \lim_{\mu\to\infty} 1-\exp\left(-\frac{\beta^2}{\sigma_1^2}\right) \\
&= \lim_{\mu\to\infty} 1-\exp\left(-\frac{1}{\sigma_1^2-1}\ln\left[\frac{(1-p)\sigma_1^2}{p}\right]\right) \\
&= \lim_{\sigma_1^2\to 1} 1-\exp\left(-\frac{1}{\sigma_1^2-1}\ln\left[\frac{(1-p)\sigma_1^2}{p}\right]\right) \\
&= 1
\end{aligned}
$$

The above steps show that asymptotically, if MAP detection is used, then as $\mu \to \infty$, the receiver will always decide that a "0" was sent. Furthermore, the probabilities decay towards their limiting value exponentially. Since the lower bound to capacity is $C \geq W\mu f(p_0, p_\alpha)$, the exponential convergence of p_0 and p_α dominates over the linear increase of $W\mu$, the lower bound to capacity decays to zero as $\mu \to \infty$. Therefore, Equations 2.3 and 2.11 are tight bounds to capacity.

2.4 Analysis of Results

The purpose of this thesis is to get an idea for what might be the optimal spreading bandwidth for a DS-CDMA system. Based on the channel model described previously in Section 2.1, a pair of asymptotically tight upper and lower bounds have been derived. Figure 2-2 is a plot, in semi-log scale, of the upper and lower bounds using parameters commonly found in a communication scenario ($W = 100\,\text{KHz}$, $\sigma_F^2 = 4$, $\gamma = 100$, $T = 0.1\,\text{sec}$, $\mathcal{E} = 20$, and $p = 0.04$). In this scenario the maximum capacity achievable with the binary signaling scheme is approximately 2.5 Mbits per second. By drawing a horizontal line from the maxima of the lower bound, it is clear that the upper bound achieves this data rate between spreading bandwidths $\mu = 6$ and

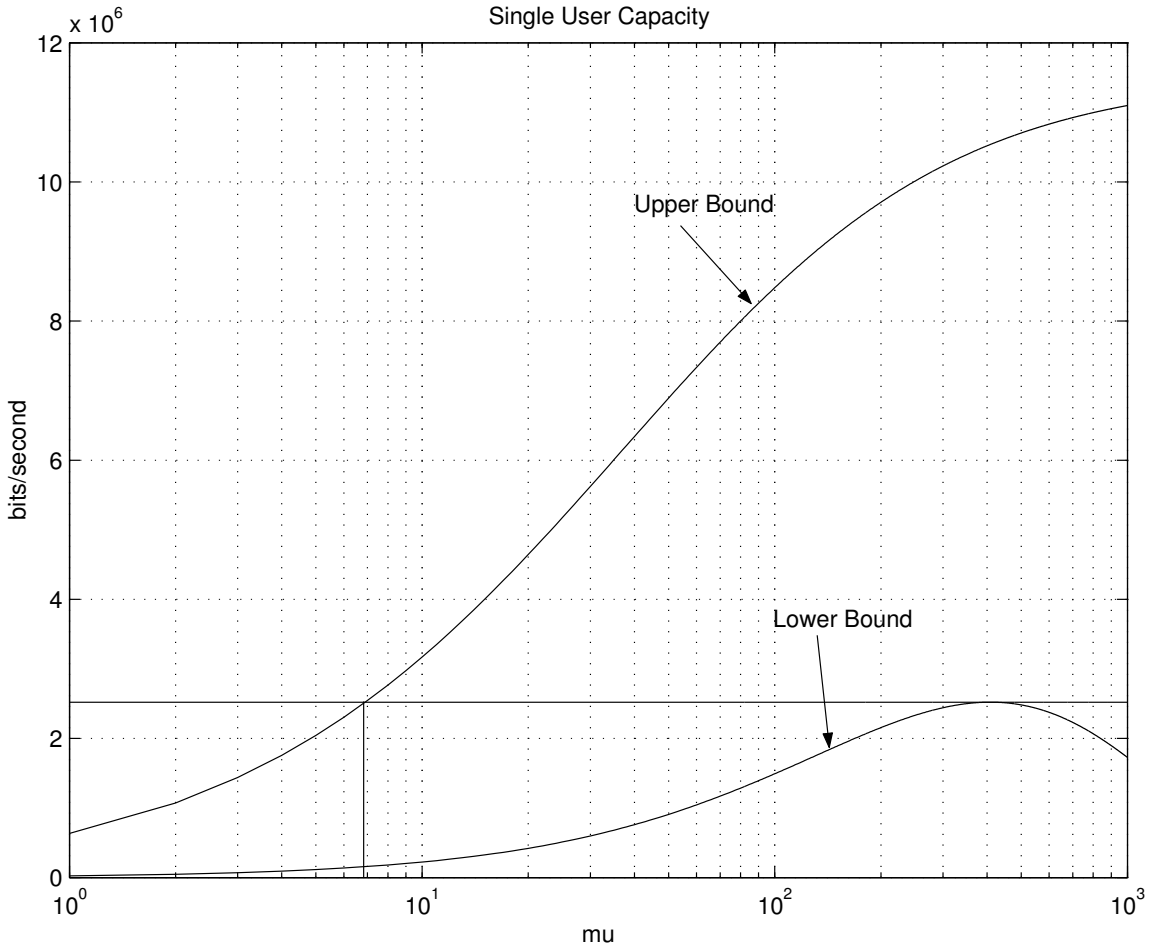

Figure 2-2: Single User Upper and Lower Bound – ($W = 100\,\mathrm{KHz}$, $\sigma_F^2 = 4$, $\gamma = 100$, $T = 0.1$ sec, $\mathcal{E} = 20$, $p = 0.04$)

$\mu = 7$ coherence bands. Therefore, it can be concluded that in a communication channel with these characteristics, the minimum spreading bandwidth should be at least $\mu = 6$ coherence bands. Because the upper bound decays very slowly, while it is theoretically possible to determine the maximum number of coherence bands to spread to, that value is so large that it is not of any practical value.

2.4.1 Effect of Varying Parameters

The upper and lower bounds to capacity are functions of the several parameters: W, $\mathcal{E}$, σ_F^2, T, γ, and p. When examining the upper and lower bounds to capacity,

these six parameters provide various degrees of freedom that can affect the optimal spreading bandwidth. Of course, the manifested results of varying these parameters are only accurate to the extend that the model was able to capture their full effects.

The Significance of p

This parameter only affects the lower bound, since in the upper bound no assumption is made about using a specific signaling scheme. In the lower bound, the parameter p is the probability that a non-zero signal is transmitted. In [16], E. Telatar showed that for energy limited Rayleigh fading channels, on-off signaling with low duty cycles should be used to approach capacity. In the context of the lower bound, the result from [16] means that p should be set as low as possible. Owing to the maximum amplitude constraint, p must satisfy:

$$\begin{aligned} \alpha = \sqrt{\frac{\mathcal{E}}{\mu p}} &\leq \frac{\gamma}{\sqrt{\mu \mathcal{E}}} \\ p &\geq \frac{\mathcal{E}^2}{\gamma^2} \end{aligned} \tag{2.17}$$

A plot of several cases of varying p (while still satisfying Equation 2.17) confirms the above hypothesis. Figure 2-3 is a plot of the upper bound versus the lower bound using several different values of p. Using the parameters $W = 100$ KHz, $\sigma_F^2 = 4$, $\gamma = 100$, $T = 0.1$ sec, $\mathcal{E} = 20$, with p varying from 0.1 to 0.04, the plots show that the highest data rate in the lower bound is achieved by $p = 0.04$, which is the smallest p that still satisfies the constraint of Equation 2.17.

p and γ

Since maximizing the data rate in the lower bound means using the lowest possible value of p, it can be seen from Equation 2.17 that the data rate increases with γ.

Variations in T

The length of the coherence time is captured by the parameter T. Normally, a longer coherence time implies less variability and greater opportunity for better channel estimation, hence the achievable rate can be expected to increase as T increases. In the signaling scheme chosen, since the binary signal for the lower bound does not use any form of channel estimation, the coherence time does not affect the achievable

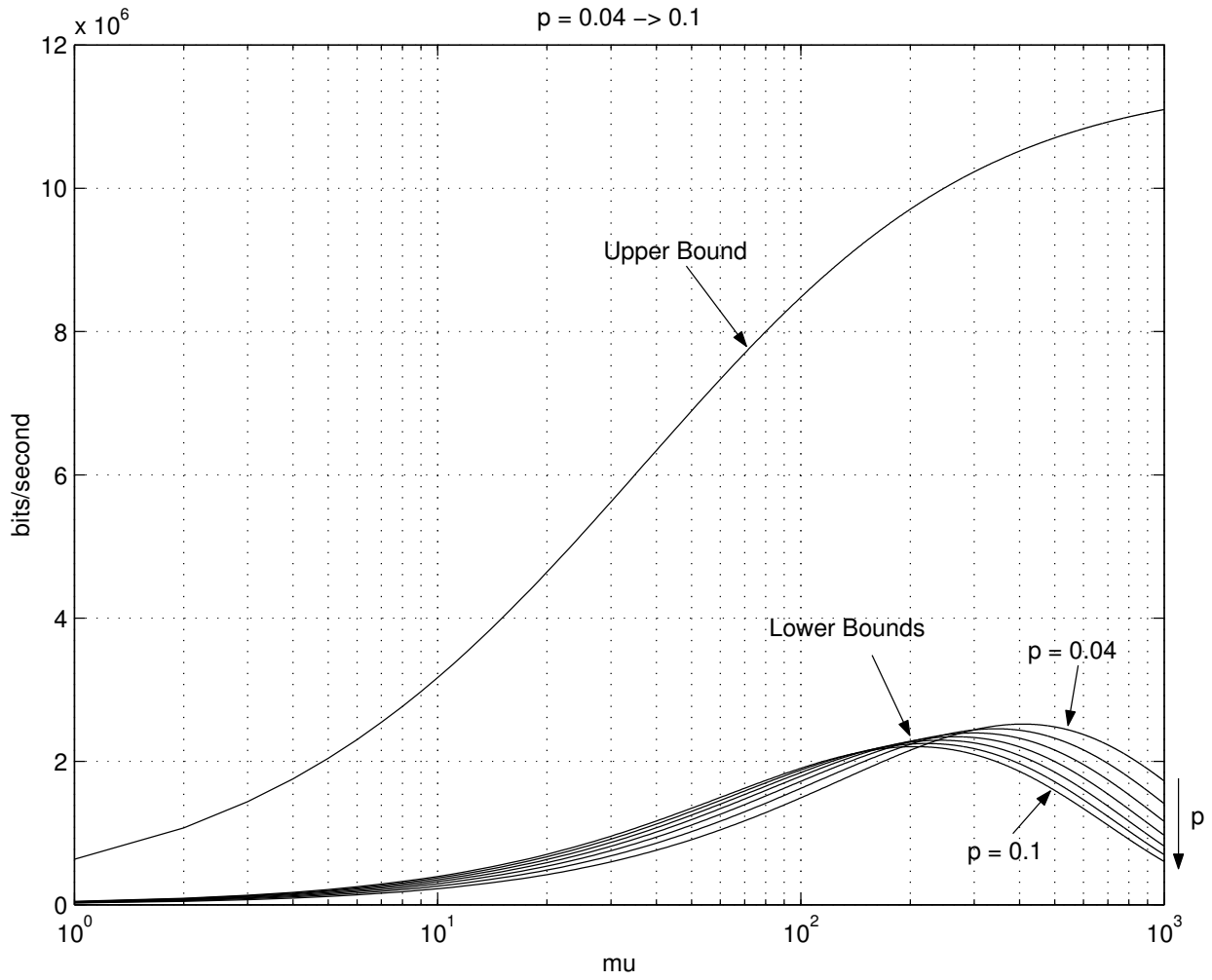

Figure 2-3: Effect on Capacity Bounds with varying p – ($W = 100\,\text{KHz}$, $\sigma_F^2 = 4$, $\gamma = 100$, $T = 0.1\,\text{sec}$, $\mathcal{E} = 20$, $p = 0.04$ to 0.1)

rate of the lower bound. In the upper bound, longer T only has minor effect on the upper limit to capacity.

Variations in W

The length of the coherence bandwidth is captured by the parameter W. Coherence bandwidth is $W \propto \frac{1}{\text{delay spread}}$, with delay spread typically on the order of microseconds (μsec). A longer coherence bandwidth implies less variability in the channel and the ability to accommodate higher data rate. Therefore, capacity should increase as the length of the coherence band increases. In the signaling scheme chosen

for the lower bound, W is only accounted for in terms of the number of samples that can be transmitted in the band, which is a linear function. In the upper bound, the equation of which is shown again below:

$$C\left(W, \mathcal{E}, \sigma_F^2, T, \mu, \gamma\right) \leq W\mu \log\left(\sigma_F^2 \frac{\mathcal{E}}{\mu} + 1\right) - \frac{\mathcal{E}^2 \mu}{\gamma^2 T} \log\left(TW \frac{\gamma^2}{\mu \mathcal{E}} \sigma_F^2 + 1\right)$$

within each coherence band, the capacity is also very nearly a linear function of W. Hence, as Figure 2-4 shows, varying W does not change the number of coherence bands μ that the system should spread to.

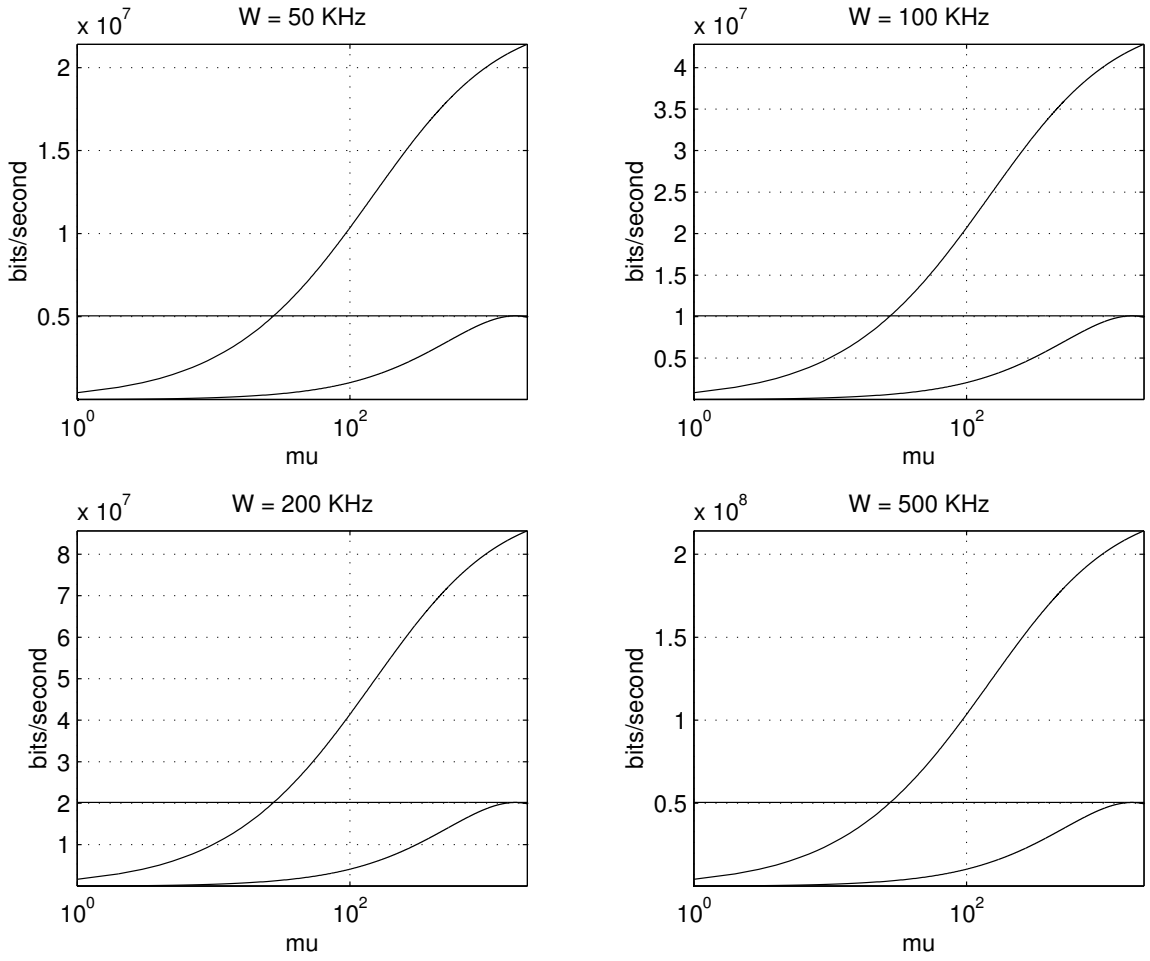

Figure 2-4: Effect on Capacity Bounds with varying W – ($W = 50\,\text{KHz} - 500\,\text{KHz}$, $\sigma_F^2 = 16$, $\gamma = 100$, $T = 0.1\,\text{sec}$, $\mathcal{E} = 20$, $p = 0.04$)

The plots in Figure 2-4 were made with the parameters $\sigma_F^2 = 16$, $\gamma = 100$, $T = 0.1$ sec, $\mathcal{E} = 20$, and $p = 0.04$. The coherence bandwidths W were varied from 50 KHz to 500 KHz. The plots, as well as examination of the output data, says that while the capacity increases linearly (or nearly so) as the coherence bandwidth W increases, the corresponding minimum number of coherence bands μ that the system should spread to remains constant at $\mu = 27$.

Variations in $\mathcal{E}$

From the examination of the effect of the parameter p, Equation 2.17 shows that the lower bound to p is directly proportional to $\mathcal{E}^2$. Because using the smallest p possible achieves the maximum data rate in the lower bound, it is logical to examine whether reduction in p achieved by a decrease in $\mathcal{E}$ can significantly increase the maximum achievable rate in the lower bound, leading to a larger minimum number of coherence bands μ to spread to. In fact, as Figure 2-5 shows, the benefits resulting from lower p does not compensate for the decrease in the achievable rate resulting from lower total average power.

The plots in Figure 2-5 were made with the parameters $W = 100$ KHz, $\sigma_F^2 = 16$, $\gamma = 100$, $T = 0.1$sec, The total average power $\mathcal{E}$ were varied from 10 to 40, with $p = \frac{\mathcal{E}^2}{\gamma^2}$. The plots, as well as examination of the output data, says that lowering $\mathcal{E}$ did not result in a higher minimum number of spreading coherence bands μ, despite having a lower p that resulted from having a lower $\mathcal{E}$. This agrees with the intuition that that in order to maximize achievable rate, use as much power as possible. However, as Equation 2.17 shows, p is a function of $\mathcal{E}^2$, and $p \leq 1$ means that $\mathcal{E} \leq \gamma$. Furthermore, as Telatar showed in [16], on-off signaling with low duty cycle should be used to approach capacity. Therefore, when $\mathcal{E} \ll \gamma$, increasing $\mathcal{E}$ is beneficial in increasing achievable rate; as $\mathcal{E}$ approaches γ, p approaches 1, and the achievable rate drops catastrophically. This is illustrated in the last plot of Figure 2-5, where $\mathcal{E} = 80$. In the upper bound, no assumptions are made about the signaling scheme used, and so increasing $\mathcal{E}$ strictly increases upper bound to capacity. Unfortunately too much power in the lower bound is detrimental to the achievable rate, and as $\mathcal{E}$ approach γ, the minimum number of coherence bands μ to spread with decreases dramatically.

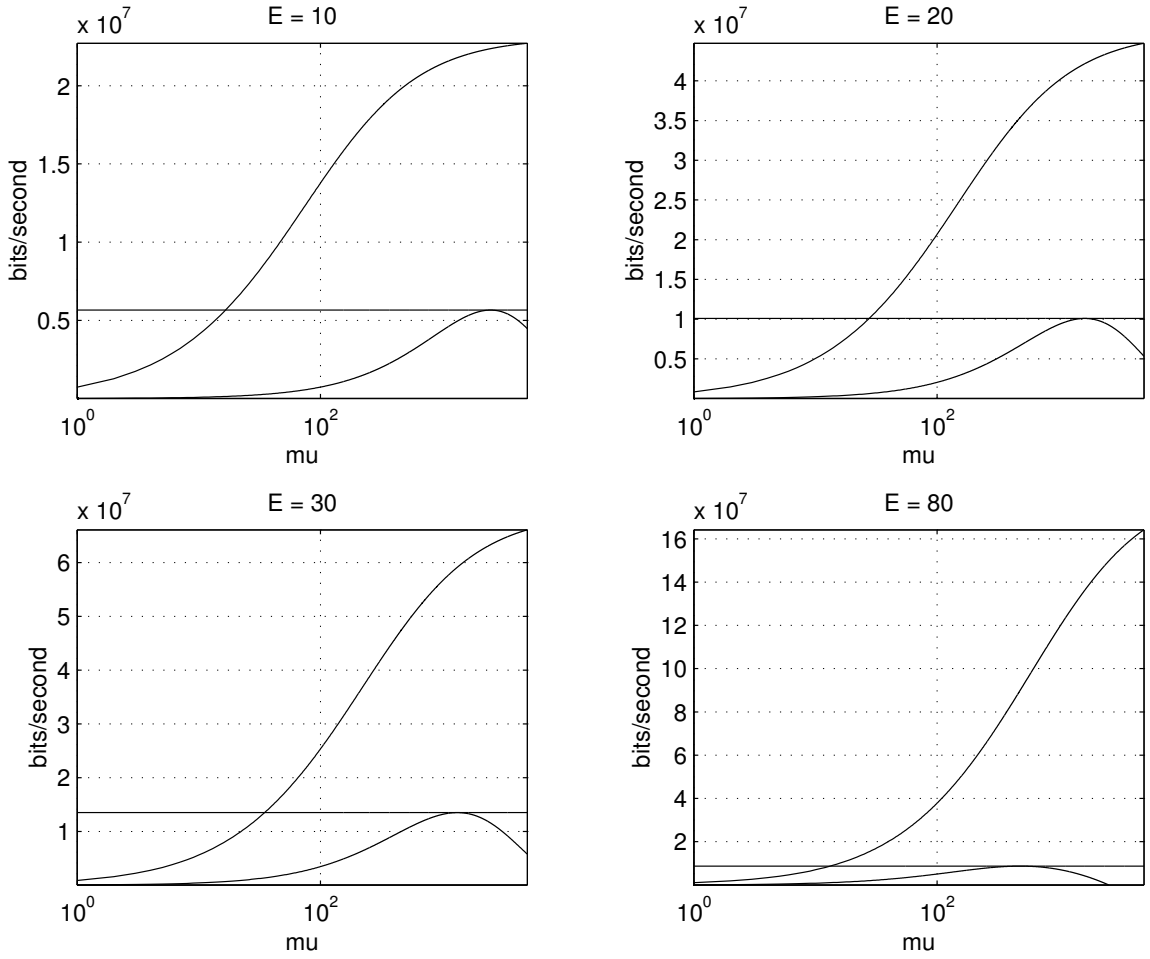

Figure 2-5: Effect on Capacity Bounds with varying $\mathcal{E}$ – ($W = 100\,\mathrm{KHz}$, $\sigma_F^2 = 16$, $\gamma = 100$, $T = 0.1\,\mathrm{sec}$, $\mathcal{E} = \{10, 20, 30, 80\}$, $p = \frac{\mathcal{E}^2}{\gamma^2}$)

The Significance of σ_F^2

$$\beta = \sqrt{\frac{\sigma_1^2}{\sigma_1^2 - 1} \ln\left[\frac{(1-p)\sigma_1^2}{p}\right]}$$

The parameter σ_F^2 represents the energy of the propagation coefficient, and is particularly significant in determining the achievable rate of the lower bound. In the lower bound, because MAP detection is used, σ_F^2 determines the detection threshold and therefore determines the crossover probabilities. As can be seen from the equation of the detection threshold β as a function of σ_F^2 (repeated above), the greater σ_F^2 is, the

easier it is for receiver to figure out which signal $X \in \{0, \alpha\}$ was sent. Therefore, the lower bound to capacity would be expected to increase significantly as σ_F^2 increases. A number of trials were run with some common parameters $W = 100\,\text{KHz}$, $\gamma = 100$, $\mathcal{E} = 20$, $T = 0.1\,\text{sec}$, and $p = 0.04$ (satisfying the constraint in Equation 2.17 with equality) with varying σ_F^2. In the top plot of Figure 2-6, the minimum number of coherence bands μ to spread to as σ_F^2 was varied, shows that there is a linear relationship between the energy of the fading coefficient σ_F^2 and minimum μ. However, since the domain of μ is the set of all positive integers, if the plot is made with sufficiently fine granularity, it will show a step-wise change as σ_F^2 is varied. The bottom plot of Figure 2-6, which uses the same parameters as the top plot, but plotted with much finer granularity, shows the staircase behavior. Nevertheless, the general trend is linear and positive.

One way to interpret this graph is to view the energy of the propagation coefficient σ_F^2 as a metric of the signal power. The ratio of σ_F^2 to additive noise power can be thought of as the fading coefficient energy to noise ratio. Since the additive noise power has already been normalized to unity, Figure 2-6 says that given the user transmits with the above parameters ($W = 100\,\text{KHz}$, $\gamma = 100$, $\mathcal{E} = 20$, $T = 0.1\,\text{sec}$, and $p = 0.04$), then the minimum number of coherence bands μ to spread is a linear function of the energy of the fading coefficient σ_F^2. As an example, for $\sigma_F^2 = 8$, the minimum number of coherence bands to spread is $\mu = 13$. Since each coherence bandwidth is of size $W = 100\,\text{KHz}$, that means given the system parameters, the system should be spread to 1.3 MHz. Considering that the commercial DS-CDMA system IS-95 transmits at a bandwidth of 1.25 MHz, these results serve as meaningful references for designing future communication systems.

Let m denote the slope of σ_F^2 vs. minimum number of spreading bandwidths μ. The plots of Figure 2-6 suggest that it may be possible to derive a closed form, analytic equation to describe m. However, it appears that a closed form analytic solution, should it exist, will be very unwieldy and would provide little additional value. A first attempt at an analytic solution may be to attempt a Taylor series expansion to simplify the lower bound. As the maxima of the lower bound occurs at

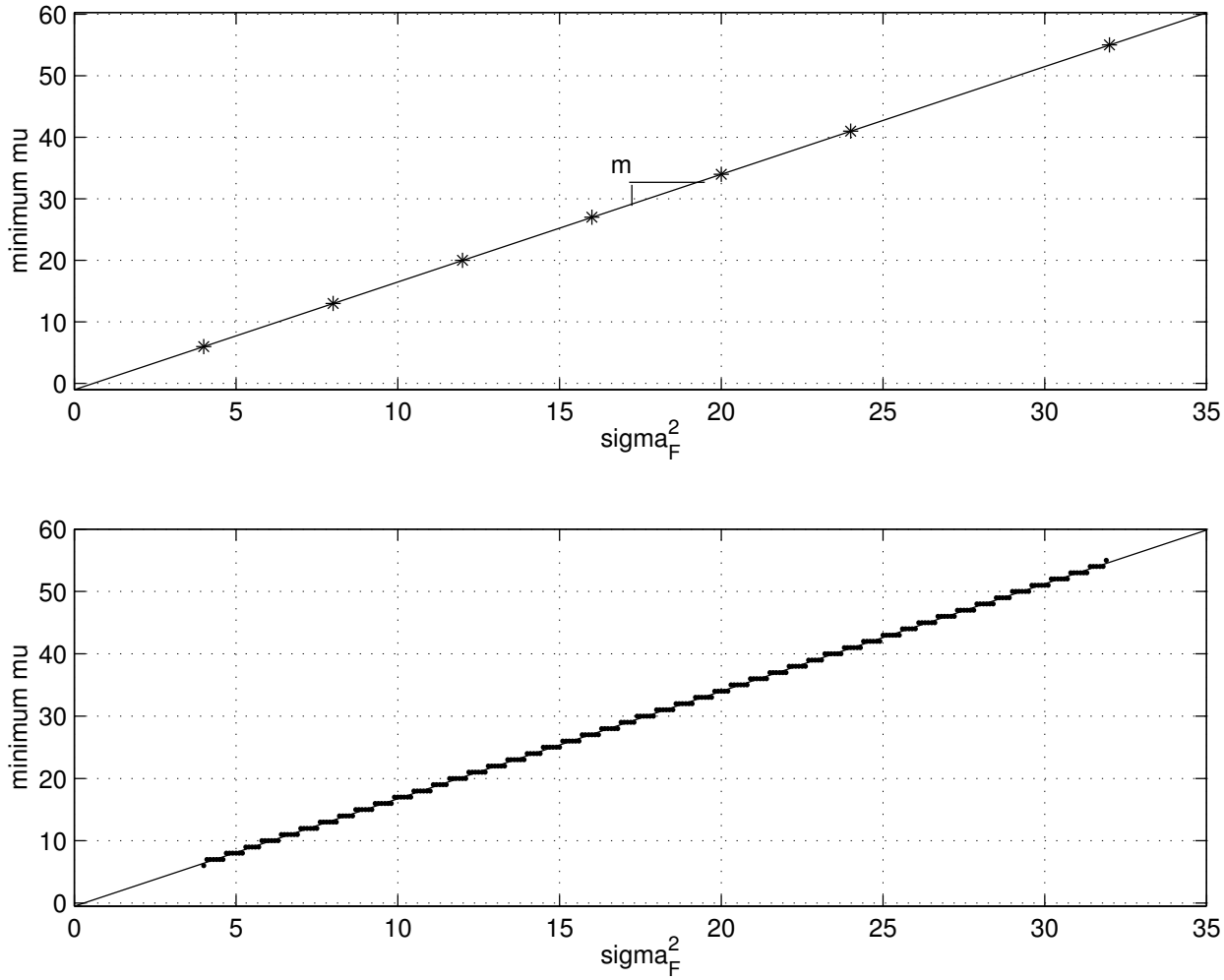

Figure 2-6: Single User: σ_F^2 vs. minimum μ

large μ, the probability of detecting an α is very small, and $r = p_Y(y = \alpha) \approx 0$. Since $r = 0$ is a singularity point of $\log r$, to attempt a Taylor series expansion runs into the problem of trying to expand around a singularity.

Statistical methods offers another possibility for arriving at a simplified expression to describe m. Since it was shown previously that the coherence bandwidth W and coherence time T does not influence the minimum number of spreading bandwidths, m is a function of $\mathcal{E}$ and γ. The plots of Figure 2-7 show that multivariate linear regression methods are not adequate for deriving an expression for $m(\mathcal{E}, \gamma)$.

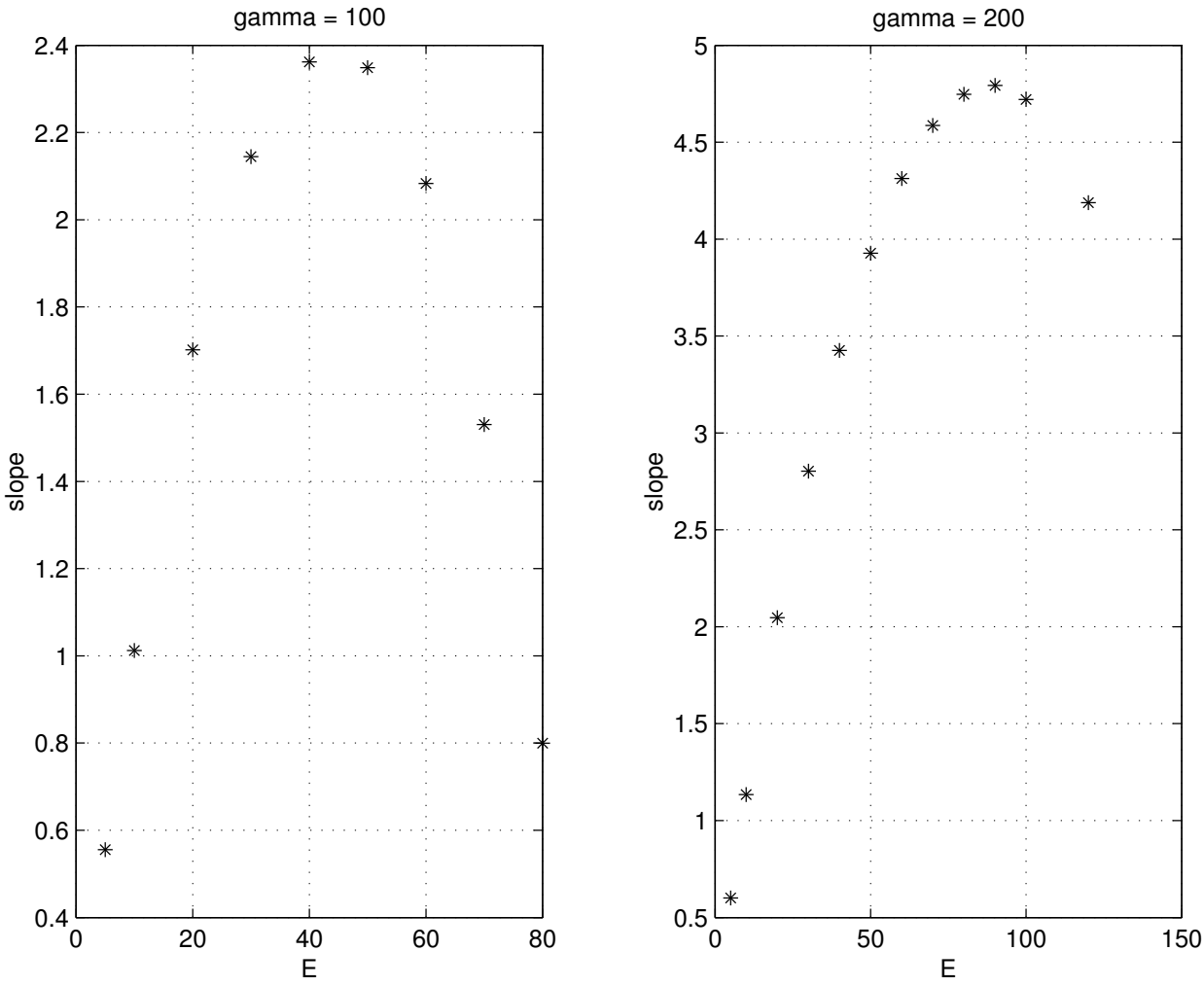

Figure 2-7: Single User: the slope m as $\mathcal{E}$ and γ is varied

Chapter 3

Analysis of Two User Multiple Access Scenario

The analysis of the single user scenario in Chapter 2 was illustrative of the basic characteristics of the system. In the typical scenario, several users simultaneously send information to the base station, and the base station receives a signal that is the sum of all the user signals. In trying to decode the signals transmitted by each user, the receiver must contend with not only environmental noise but also interference from other users as well. The multiple access scenario in Additive White Gaussian Noise (AWGN) channel has been thoroughly studied, and is well understood ([2], [8], [3]). This chapter will perform an analogous examination of the multiple access case in a fading environment. A basic illustration of the multiple access scenario can be obtained by an examination of the simple two user case.

3.1 Channel Model

The channel model for this two user scenario is the same as that for the single user scenario detailed in Section 2.1. Each user experiences independent Rayleigh flat fading, whose random multiplicative propagation coefficient is modeled as a zero mean, complex circularly symmetric Gaussian random variable, with variance σ_F^2. At the receiver, the sum of the user signals are further corrupted by an additive noise that is

Parameter	Description	Constraints/Distribution
W	coherence bandwidth size	
μ	number of coherence bands	$\mu \in \{\text{positive integers}\}$
ε	total average power	
T	length of coherence time	
γ	peakiness of the signal	
$F[i]$	propagation coefficient in coherence band i	$F[i]$ is zero mean, circularly symmetric, complex Gaussian. $E[F^2] = \sigma_F^2$
$X[i]_j$	input at sample time j in coherence band i	$E[X^2] \leq \frac{\varepsilon}{\mu}$ $\lvert X \rvert \leq \frac{\gamma}{\varepsilon}\sqrt{E[X^2]} = \frac{\gamma}{\sqrt{\varepsilon\mu}}$
$Z[i]_j$	noise at sample time j in coherence band i	$Z[i]_j$ is zero mean, circularly symmetric, complex with normalized unit variance

Table 3.1: Summary of Channel Model Parameters

also modeled as zero mean, complex circularly symmetric Gaussian random variable, but with normalized unit variance. Each channel over distinct coherence bandwidths are independent, and transmission occurs over μ distinct coherence bandwidths. The propagation coefficient for each coherence bandwidth remains constant for T, the coherence time, after which it changes to a new independent value.

Each user is subject to the same constraints (e.g. the variance of the propagation coefficient are both σ_F^2), and independence between the parameters (modeled as random variables) associated with different users are assumed. The users transmit within the same number of coherence bands μ, each of size W hertz. The signals are sampled at the Nyquist rate of W samples per second. Thus within the coherence time T there are a total of TW samples and the received vector in the i^{th} coherence band over the j^{th} coherence time is:

$$Y[i]_{jTW+1}^{(j+1)TW} = F_1[i]_j X_1[i]_{jTW+1}^{(j+1)TW} + F_2[i]_j X_2[i]_{jTW+1}^{(j+1)TW} + Z[i]_{jTW+1}^{(j+1)TW} \tag{3.1}$$

Each user is subject to the same average power constraint and peakiness constraint imposed on the $X[i]_j's$. Thus a limited amount of power ε is distributed equally to each of the μ coherence bands, yielding an upper bound on the second moment given by

$E\left[X[i]_j^2\right] \leq \frac{\varepsilon}{\mu}$. The peak amplitude is upper bounded by $|X| \leq \frac{\gamma}{\varepsilon}\sqrt{E\left[X[i]_j^2\right]}$, where γ is the peakiness of the signal. The relevant channel parameters are summarized in Table 3.1.

3.2 Upper Bound to Wideband Capacity

Based on the channel model, within each coherence band, each user has an average power constraint corresponding to an upper bound on the second moment of the signal. However, only signals which satisfy the second moment constraint with equality can achieve the upper bound to capacity. The capacity region of a multiple access channel is the closure of the convex hull of the set of points (C_1, C_2) satisfying:

$$\begin{aligned} C_1 &\leq I(\underline{X}_1; \underline{Y}|\underline{X}_2) \\ C_2 &\leq I(\underline{X}_2; \underline{Y}|\underline{X}_1) \\ C_1 + C_2 &\leq I(\underline{X}_1, \underline{X}_2; \underline{Y}) \end{aligned}$$

Keeping that in mind, Lemma 3 gives the capacity region of the upper bound in the two user scenario.

Lemma 3 *The upper bound to wideband capacity for the two user scenario based on the channel model described previously in Section 3.1 is:*

$$C_1 \leq W\mu \log\left(\sigma_F^2 \frac{\mathcal{E}}{\mu} + 1\right) - \frac{\mathcal{E}^2}{\gamma^2 T} \log\left(TW \frac{\gamma}{\sqrt{\mu\mathcal{E}}}\sigma_F^2 + 1\right) \tag{3.2}$$

$$C_2 \leq W\mu \log\left(\sigma_F^2 \frac{\mathcal{E}}{\mu} + 1\right) - \frac{\mathcal{E}^2}{\gamma^2 T} \log\left(TW \frac{\gamma}{\sqrt{\mu\mathcal{E}}}\sigma_F^2 + 1\right) \tag{3.3}$$

$$C_1 + C_2 \leq W\mu \log\left(2\sigma_F^2 \frac{\mathcal{E}}{\mu} + 1\right) - \frac{\mathcal{E}^2}{\gamma^2 T} \log\left(2TW \frac{\gamma}{\sqrt{\mu\mathcal{E}}}\sigma_F^2 + 1\right) \tag{3.4}$$

Proof:

The proof to Equations 3.2 and 3.3 is as follows:

$$
\begin{aligned}
C_1 &= \lim_{k\to\infty} \max_{p_X} \left(\frac{1}{k} \sum_{j=1}^{k} \sum_{i=1}^{\mu} \frac{1}{T} I(\underline{X}_1[i]_{jTW+1}^{(j+1)TW}; \underline{Y}[i]_{jTW+1}^{(j+1)TW} \mid \underline{X}_2[i]_{jTW+1}^{(j+1)TW}) \right) \\
&= \lim_{k\to\infty} \max_{p_X} \frac{1}{k} \sum_{j=1}^{k} \sum_{i=1}^{\mu} \frac{1}{T} \Big[h(\underline{X}_1[i]_{jTW+1}^{(j+1)TW} \mid \underline{X}_2[i]_{jTW+1}^{(j+1)TW}) \\
&\quad - h(\underline{X}_1[i]_{jTW+1}^{(j+1)TW} \mid \underline{X}_2[i]_{jTW+1}^{(j+1)TW}, \underline{Y}[i]_{jTW+1}^{(j+1)TW}) \Big] \\
&\overset{a}{\leq} \lim_{k\to\infty} \max_{p_X} \frac{1}{k} \sum_{j=1}^{k} \sum_{i=1}^{\mu} \frac{1}{T} \Big[h(\underline{X}_1[i]_{jTW+1}^{(j+1)TW} \mid F_2, \underline{X}_2[i]_{jTW+1}^{(j+1)TW}) \\
&\quad - h(\underline{X}_1[i]_{jTW+1}^{(j+1)TW} \mid F_2, \underline{X}_2[i]_{jTW+1}^{(j+1)TW}, \underline{Y}[i]_{jTW+1}^{(j+1)TW}) \Big] \\
&= \lim_{k\to\infty} \max_{p_X} \left(\frac{1}{k} \sum_{j=1}^{k} \sum_{i=1}^{\mu} \frac{1}{T} I(\underline{X}_1[i]_{jTW+1}^{(j+1)TW}; \underline{Y}[i]_{jTW+1}^{(j+1)TW} \mid F_2, \underline{X}_2[i]_{jTW+1}^{(j+1)TW}) \right) \\
&= \lim_{k\to\infty} \max_{p_X} \left(\frac{1}{k} \sum_{j=1}^{k} \sum_{i=1}^{\mu} \frac{1}{T} I(\underline{X}_1[i]_{jTW+1}^{(j+1)TW}; F_1 \underline{X}_1[i]_{jTW+1}^{(j+1)TW} + \underline{Z}[i]_{jTW+1}^{(j+1)TW}) \right) \\
&\overset{b}{\leq} W\mu \log\left(\sigma_F^2 \frac{\mathcal{E}}{\mu} + 1 \right) - \frac{\mathcal{E}^2 \mu}{\gamma^2 T} \log\left(TW \frac{\gamma^2}{\mu \mathcal{E}} \sigma_F^2 + 1 \right)
\end{aligned}
$$

(a) follows from the properties of conditional entropy:

$$
\begin{aligned}
& & & \text{because } X_1, X_2, \text{ and } F_2 \text{ are independent} \\
h(\underline{X}_1|\underline{X}_2) = h(\underline{X}_1|F_2, \underline{X}_2) &= & h(\underline{X}_1) \\
& & & \text{similarly, because conditioning} \\
& & & \text{does not increase entropy} \\
h(\underline{X}_1|\underline{Y}, \underline{X}_2) &\geq & h(\underline{X}_1|F_2, \underline{Y}, \underline{X}_2) \\
\text{therefore } I(\underline{X}_1, \underline{Y}|\underline{X}_2) &\leq & I(\underline{X}_1, \underline{Y}|F_2, \underline{X}_2)
\end{aligned}
$$

(b) follows from the same line as that given in the proof of **Lemma 1**.

The proof for C_2 of Equation 3.3 follows by symmetry. To prove Equation 3.4, begin with the definition of capacity as mutual information.

$$
C_1 + C_2 = \lim_{k\to\infty} \max_{p_X} \left(\frac{1}{k} \sum_{j=1}^{k} \sum_{i=1}^{\mu} \frac{1}{T} I(\underline{X}_1[i]_{jTW+1}^{(j+1)TW}, \underline{X}_2[i]_{jTW+1}^{(j+1)TW}; \underline{Y}[i]_{jTW+1}^{(j+1)TW}) \right) \quad (3.5)
$$

The fourth central moment of $X[i]_j$ is $\frac{\gamma}{\mu^2}$ and its average power constraint is $\frac{\mathcal{E}}{\mu}$. Since there are no sender channel side information and all the bandwidth slices are independent, applying the concavity of mutual information in the input distribution results in selecting all the inputs to be IID to maximize the righthand side (RHS) of Equation 3.5.

First rewrite mutual information in terms of entropy:

$$\begin{aligned} & \frac{1}{T} I(\underline{X}_1[i]_{jTW+1}^{(j+1)TW}, \underline{X}_2[i]_{jTW+1}^{(j+1)TW}; \underline{Y}[i]_{jTW+1}^{(j+1)TW}) \\ = \; & \frac{1}{T} h(\underline{Y}[i]_{jTW+1}^{(j+1)TW}) - \frac{1}{T} h(\underline{Y}[i]_{jTW+1}^{(j+1)TW} \mid \underline{X}_1[i]_{jTW+1}^{(j+1)TW}, \underline{X}_2[i]_{jTW+1}^{(j+1)TW}) \end{aligned} \tag{3.6}$$

Now find a suitable upper bound to Equation 3.6. First upper bound $h(\underline{Y})$

$$\begin{aligned} \frac{1}{T} h(\underline{Y}[i]_{jTW+1}^{(j+1)TW}) &\overset{a}{\leq} \frac{1}{T} \log\left((\pi e)^{TW} |\Lambda_{\underline{Y}[i]_{jTW+1}^{(j+1)TW}}| \right) \qquad (3.7) \\ &\overset{b}{\leq} \frac{1}{T} \log\left((\pi e)^{TW} \prod_{m=1}^{TW} \left[\sigma_F^2 (\sigma_{X_{1,m}}^2 + \sigma_{X_{2,m}}^2) + 1 \right] \right) \\ &= \log(\pi e) + \frac{1}{T} \sum_{m=1}^{TW} \log\left[\sigma_F^2 (\sigma_{X_{1,m}}^2 + \sigma_{X_{2,m}}^2) + 1 \right] \\ &\overset{c}{\leq} W \log(\pi e) + W \log\left(2\sigma_F^2 \frac{\mathcal{E}}{\mu} + 1 \right) \qquad (3.8) \end{aligned}$$

(a) follows because entropy is maximized by a Gaussian distribution for a given covariance matrix. Equation 3.7, which gives the entropy of a zero mean, complex circularly symmetric Gaussian random vector, follows from Lemma 6 given in Appendix A.

(b) follows from Hadamard's inequality [3].

(c) follows from the average power constraint of the channel model.

Next find a suitable lower bound to $h(\underline{Y}|\underline{X}_1, \underline{X}_2)$

$$\begin{aligned} & \frac{1}{T} h\left(\underline{Y}[i]_{jTW+1}^{(j+1)TW} \mid \underline{X}_1[i]_{jTW+1}^{(j+1)TW}, \underline{X}_2[i]_{jTW+1}^{(j+1)TW} \right) \\ \overset{a}{=} \; & \frac{1}{T} E_X \left[\log\left((\pi e)^{TW} |\Lambda_{\underline{Y}[i]_{jTW+1}^{(j+1)TW} | \underline{X}_1[i]_{jTW+1}^{(j+1)TW}, \underline{X}_2[i]_{jTW+1}^{(j+1)TW}}| \right) \right] \end{aligned}$$

$$\begin{aligned} &\overset{b}{\geq} \frac{1}{T} E_X \left[\log \left((\pi e)^{TW} \left[\sigma_F^2 (\|\underline{X}_1\|^2 + \|\underline{X}_2\|^2) + 1 \right] \right) \right] \\ &= W \log(\pi e) + \frac{1}{T} E_X \left[\log \left(\sigma_F^2 (\|\underline{X}_1\|^2 + \|\underline{X}_2\|^2) + 1 \right) \right] \end{aligned} \tag{3.9}$$

(a) results from the fact that conditioned on $\underline{X}_1[i]_{jTW+1}^{(j+1)TW}$ and $\underline{X}_2[i]_{jTW+1}^{(j+1)TW}$, $\underline{Y}[i]_{jTW+1}^{(j+1)TW}$ is a zero mean, complex circularly symmetric Gaussian random vector.

(b) follows from taking the determinant of the conditional covariance matrix, which is given by the following:

$$\Lambda_{\underline{Y}|\underline{X}_1,\underline{X}_2} \begin{bmatrix} \sigma_F^2 \left(x_1[1]^2 + x_2[1]^2 \right) + 1 & \sigma_F^2 \left(x_1[1]x_1[2] + x_2[1]x_2[2] \right) & \cdots & \sigma_F^2 \left(x_1[1]x_1[n] + x_1[1]x_1[n] \right) \\ \sigma_F^2 \left(x_1[2]x_1[1] + x_2[2]x_2[1] \right) & \sigma_F^2 \left(x_1[2]^2 + x_2[2]^2 \right) + 1 & \cdots & \sigma_F^2 \left(x_1[2]x_1[n] + x_2[2]x_2[n] \right) \\ \vdots & \vdots & \ddots & \vdots \\ \sigma_F^2 \left(x_1[n]x_1[1] + x_2[n]x_2[1] \right) & \sigma_F^2 \left(x_1[n]x_1[2] + x_2[n]x_2[2] \right) & \cdots & \sigma_F^2 \left(x_1[n]^2 + x_2[n]^2 \right) + 1 \end{bmatrix}$$

the eigenvalues of $\Lambda_{\underline{Y}[i]_{jTW+1}^{(j+1)TW}|\underline{X}[i]_{jTW+1}^{(j+1)TW}}$ can be obtained using Lemma 8, given in Appendix A. Taking the product the eigenvalues gives the resulting determinant:

$$\begin{aligned} |\Lambda_{\underline{Y}|\underline{X}_1,\underline{X}_2}| &= \sigma_F^2 \left(\|\underline{X}_1\|^2 + \|\underline{X}_2\|^2 \right) + 1 \\ &\quad + \sigma_F^2 \sigma_F^2 \left(\sum_{k=1}^{TW-1} \sum_{l=k+1}^{TW} (x_1[k]x_2[l] - x_1[l]x_2[k])^2 \right) \\ &\quad \text{which can be upper bounded as:} \\ |\Lambda_{\underline{Y}|\underline{X}_1,\underline{X}_2}| &\geq \sigma_F^2 \left(\|\underline{X}_1\|^2 + \|\underline{X}_2\|^2 \right) + 1 \end{aligned}$$

Any particular signaling scheme would constitute a valid lower bound to capacity so long as it satisfied the conditions outlined in the channel model. Therefore, a suitable lower bound to Equation 3.9 can be obtained by using a binary signal constellation that satisfies the second moment constraint with equality and and subject to the peak amplitude constraint. X is therefore distributed as follows:

$$X = \begin{cases} 0 & \text{with prob. } 1 - \frac{\mathcal{E}^2}{\gamma^2} \\ \frac{\gamma}{\sqrt{\mu \mathcal{E}}} & \text{with prob. } \frac{\mathcal{E}^2}{\gamma^2} \end{cases}$$

thus, using this distribution and applying the concavity of the log function, Equation 3.9 can be lower bounded as:

$$\begin{aligned} & \frac{1}{T} h(\underline{Y}[i]_{jTW+1}^{(j+1)TW} \mid \underline{X}_1[i]_{jTW+1}^{(j+1)TW}, \underline{X}_2[i]_{jTW+1}^{(j+1)TW}) \\ \geq \; & W \log(\pi e) + \frac{\mathcal{E}^2}{T\gamma^2} \log\left(2TW \frac{\gamma^2}{\mu\mathcal{E}} \sigma_F^2 + 1\right) \end{aligned} \tag{3.10}$$

Substituting Equations 3.8 and 3.10 into Equation 3.6 and taking the limit in Equation 3.5 yields the desired result. ***Q.E.D***

3.2.1 Tightness of the Upper Bound

Now verify that the asymptotic behavior of the upper bounds just derived does, in the limit as $\mu \to \infty$, approach zero just as in the single user case. It was already shown in Section 2.2 that the bounds given by Equations 3.2 and 3.3 are asymptotically tight. In a similar manner, it can be shown that in the limit of infinite bandwidth, the upper bound to capacity given by Equation 3.4 approaches zero:

$$\begin{aligned} & \lim_{\mu\to\infty} W\mu \log\left(2\sigma_F^2 \frac{\varepsilon}{\mu} + 1\right) - \frac{\varepsilon^2\mu}{\gamma^2 T} \log\left(2TW \frac{\gamma^2}{\mu\varepsilon} \sigma_F^2 + 1\right) \\ & \text{let } x = \tfrac{1}{\mu} \text{ and applying L'Hospital's rule:} \\ = \; & \lim_{x\to 0^+} \frac{W}{x} \log\left(2\sigma_F^2 \varepsilon x + 1\right) - \frac{\varepsilon^2}{\gamma^2 T x} \log\left(2TW \frac{\gamma^2 x}{\varepsilon} \sigma_F^2 + 1\right) \\ = \; & \lim_{x\to 0^+} \frac{2W\sigma_F^2\varepsilon}{2\sigma_F^2\varepsilon x + 1} - \frac{2W\sigma_F^2\varepsilon}{2TW\frac{\gamma^2\sigma_F^2}{\varepsilon} x + 1} \\ = \; & 2W\sigma_F^2\varepsilon - 2W\sigma_F^2\varepsilon \\ = \; & 0 \end{aligned}$$

3.3 Lower Bound to Wideband Capacity

Like the single user scenario, the upper bound to wideband capacity in the two user case provides little information by itself. Having derived the upper bound, it is now necessary to develop an appropriate lower bound. For the sake of simplicity, as well

as ease of comparison to the single user case, the binary signaling scheme developed in Section 2.3.1 can be transplanted and used for this multiple access scenario. The general idea of the scheme in Section 2.3.1 remains the same, however, the nature of multiple access introduces issues and problems that must be accounted for.

3.3.1 The Binary Signaling Scheme

As in the single user case, the binary signaling scheme also be used here. Just as in the upper bound, let the $X[i]_j$'s be chosen IID, and $X[i]_j \in \{0, \alpha\}$ with the following distribution:

$$X = \begin{cases} 0 & \text{with prob. } 1-p \\ \alpha = \sqrt{\frac{\varepsilon}{\mu p}} \leq \frac{\gamma}{\sqrt{\mu\varepsilon}} & \text{with prob. } p \end{cases} \tag{3.11}$$

The above distribution satisfies the second moment constraint with equality, and keeping the peak amplitude constraint in mind, the peakiness $\gamma \geq \frac{\varepsilon}{\sqrt{p}}$. Because γ does not directly factor into the second moment constraint, varying γ in this distribution gives one extra degree of freedom in adjusting the resulting achievable rate. Since this is a multiple access scenario, the received signal is the sum of all the user signal, each corrupted by their independent fading coefficient, plus the additive Gaussian noise.

$$Y[i]_j = F_1[i]X_1[i]_j + F_2[i]X_2[i]_j + Z[i]_j$$

Once transmitted, the receiver performs MAP detection to recover the transmitted signal. In attempting to decode a particular user's signal, the receiver accounts for the presence of the other user by treating its signal as noise. Lemma 4 gives the lower bound to capacity.

Lemma 4 *The lower bound to wideband capacity based on the channel model described in Section 3.1 and the particular signaling scheme with MAP detection given in Section 3.3.1 is:*

$$C\left(W, \mathcal{E}, \sigma_F^2, T, \mu, \gamma, p\right) \;\geq\; W\mu\left[(1-r)\log\frac{1}{1-r} + r\log\frac{1}{r}\right]$$

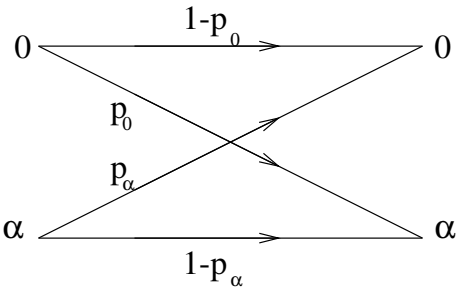

Figure 3-1: Discrete Binary Channel with cross-over probabilities p_0 and p_α

$$
\begin{aligned}
& - W\mu\,(1-p)\,\left[(1-p_0)\log\frac{1}{1-p_0} + p_0\log\frac{1}{p_0}\right] \\
& - W\mu\,p\,\left[(1-p_\alpha)\log\frac{1}{1-p_\alpha} + p_\alpha\log\frac{1}{p_\alpha}\right] \qquad (3.12)
\end{aligned}
$$

where

$$
\begin{aligned}
p_0 &= (1-p)\exp\left(-\beta^2\right) + p\exp\left(-\frac{\beta^2}{\sigma_1^2}\right) \\
p_\alpha &= (1-p)\left(1-\exp\left(-\frac{\beta^2}{\sigma_1^2}\right)\right) + p\left(1-\exp\left(-\frac{\beta^2}{\sigma_2^2}\right)\right) \\
r &= (1-p)p_0 + p(1-p_\alpha) \\
\beta^2 &= \frac{\sigma_2^2}{\sigma_2^2-1}\ln\left[\frac{(1-p)^2\sigma_2^2}{p^2}\right] \\
\sigma_1^2 &= \frac{\mathcal{E}}{\mu p}\sigma_F^2 + 1 \\
\sigma_2^2 &= 2\frac{\mathcal{E}}{\mu p}\sigma_F^2 + 1
\end{aligned}
$$

Proof:

During transmission through the communication channel the signal is corrupted by the multiplicative and additive noise. Applying MAP detection reduces the channel into a discrete binary channel with cross-over probabilities p_0 and p_α, as shown in Figure 3-1.

Let $CN(0,\sigma^2)$ represent the PDF of a zero mean, complex circularly symmetric Gaussian random variable with variance σ^2.

$$f_X(x) = CN(0,\sigma^2) = \frac{1}{\pi\sigma^2}\exp\left(-\frac{|x|^2}{\sigma^2}\right)$$

Unlike the single user case, the additive noise in this case is the sum of additive receiver noise plus the corruption that results from the presence of the other user's signal. Let $\tilde{Z}[i]_j$ be the sum of the contributing additive noise effects, then for a receiver trying to decode **user one's** signal:

$$\begin{aligned}
Y[i]_j &= F_1 X_1[i]_j + \tilde{Z}[i]_j \\
&\quad \text{where } \tilde{Z}[i]_j \text{ is the sum of additive} \\
&\quad \text{receiver noise and the other user's signal} \\
\tilde{Z}[i]_j &= Z[i]_j + F_2 X_2[i]_j \\
&= (1-p) f_{\tilde{Z}}(\tilde{z}|x=0) + p f_{\tilde{Z}}(\tilde{z}|x=\alpha) \\
&= (1-p) CN(0,1) + p\, CN(0, \alpha^2\sigma_F^2 + 1) \\
&\quad \text{let } \sigma_1^2 = \alpha^2\sigma_F^2 + 1 \\
&= (1-p) CN(0,1) + p\, CN(0, \sigma_1^2)
\end{aligned}$$

Given user one sent a "0", the distribution of the received signal is:

$$f_{Y|X_1}(y|x_1=0) = (1-p) CN(0,1) + p\, CN(0,\sigma_1^2)$$

Given user one sent an "α", the distribution of the received signal is

$$\begin{aligned}
f_{Y|X_1}(y|x_1=\alpha) &= (1-p) CN(0,\sigma_1^2) + p\, CN(0, 2\alpha^2\sigma_F^2 + 1) \\
&\quad \text{let } \sigma_2^2 = 2\alpha^2\sigma_F^2 + 1 \\
&= (1-p) CN(0,\sigma_1^2) + p\, CN(0,\sigma_2^2)
\end{aligned}$$

Because of the circular symmetry of the PDF, the detection threshold is determined solely by its magnitude and can be calculated by solving the following equations:

$$\begin{aligned}
(1-p) f_{Y|X_1}(y|x_1=0) &= p\, f_{Y|X_1}(y|x_1=\alpha) \\
(1-p)\left((1-p) CN(0,1) + p\, CN(0,\sigma_1^2)\right) &= p\left((1-p) CN(0,\sigma_1^2) + p\, CN(0,\sigma_2^2)\right)
\end{aligned}$$

$$
\begin{aligned}
(1-p)^2 CN(0,1) &= p^2 CN(0,\sigma_2^2) \\
(1-p)^2 \frac{1}{\pi}\exp\left(-|y|^2\right) &= p^2 \frac{1}{\pi\sigma_2^2}\exp\left(-\frac{|y|^2}{\sigma_2^2}\right) \\
\text{solving the above equation} & \\
|y| &= \sqrt{\frac{\sigma_2^2}{\sigma_2^2-1}\ln\left[\frac{\sigma_2^2(1-p)^2}{p^2}\right]} \qquad (3.13)
\end{aligned}
$$

The detection threshold based solely on the **magnitude** of the received complex signal is that given in Equation 3.13.

Having determined the detection threshold as given in Equation 3.13, the crossover probabilities can be calculated by integrating over the corresponding decision regions. Since only the magnitude factors into the decision regions, the the conditional PDF of the **magnitude** ϱ of the received signal, by a simple change of variable plus accounting for the phase, is the scaled sum of Rayleigh distributed random variables given by the following:

$$
\begin{aligned}
f_{\varrho|X}(\varrho|x=0) &= (1-p)(2\varrho)\exp\left(-\varrho^2\right) + p\left(\tfrac{2\varrho}{\sigma_1^2}\right)\exp\left(-\tfrac{\varrho^2}{\sigma_1^2}\right) \quad \text{for } \varrho \geq 0 \\
f_{\varrho|X}(\varrho|x=\alpha) &= (1-p)\left(\tfrac{2\varrho}{\sigma_1^2}\right)\exp\left(-\tfrac{\varrho^2}{\sigma_1^2}\right) + p\left(\tfrac{2\varrho}{\sigma_2^2}\right)\exp\left(-\tfrac{\varrho^2}{\sigma_2^2}\right) \quad \text{for } \varrho \geq 0
\end{aligned}
$$

Let β be the detection threshold given by Equation 3.13, the crossover probabilities p_0 and p_α are:

$$
\begin{aligned}
\beta^2 &= \frac{\sigma_2^2}{\sigma_2^2-1}\ln\left[\frac{\sigma_2^2(1-p)^2}{p^2}\right] \\
p_0 &= \int_\beta^\infty f_{\varrho|X}(\varrho|x=0)\,d\varrho \\
&= (1-p)\exp\left(-\beta^2\right) + p\,\exp\left(-\frac{\beta^2}{\sigma_1^2}\right) \qquad (3.14) \\
p_\alpha &= \int_0^\beta f_{\varrho|X}(\varrho|x=\alpha)\,d\varrho \\
&= (1-p)\left(1-\exp\left(-\frac{\beta^2}{\sigma_1^2}\right)\right) + p\,\left(1-\exp\left(-\frac{\beta^2}{\sigma_2^2}\right)\right) \qquad (3.15)
\end{aligned}
$$

Given the crossover probabilities, the probability r of receiving an α can be easily

calculated:

$$
\begin{aligned}
r = p_Y(y=\alpha) &= (1-p)p_0 + (1-p_\alpha)p \qquad (3.16)\\
&\text{substituting in Equations 3.14 and 3.15}\\
r &= (1-p)\left[(1-p)\exp\left(-\beta^2\right) + p\exp\left(-\frac{\beta^2}{\sigma_1^2}\right)\right] +\\
&\quad p - p(1-p)\left(1-\exp\left(-\frac{\beta^2}{\sigma_1^2}\right)\right) -\\
&\quad p^2\left(1-\exp\left(-\frac{\beta^2}{\sigma_2^2}\right)\right)
\end{aligned}
$$

The mutual information of a single use of the discrete binary channel is given by:

$$
\begin{aligned}
I(Y;X) &= H(Y) - H(Y|X)\\
&\text{for a discrete binary distribution}\\
&\text{with probabilities } a \text{ and } 1-a, \text{ let}\\
H(a) &= a\log\frac{1}{a} + (1-a)\log\frac{1}{1-a}\\
&\text{therefore, for a single use of the channel}\\
I(Y;X) &= H(r) - E_x\left[H(Y|X=x)\right]\\
&= H(r) - pH(p_\alpha) - (1-p)H(p_0) \qquad (3.17)
\end{aligned}
$$

Substituting r, p_0, p_α from Equations 3.16, 3.14, and 3.15, respectively, into Equation 3.17, and multiplying by $W\mu$ to account for the $W\mu$ uses of the channel per second yields the capacity in bits/second as given in Equation 3.12. ***Q.E.D.***

3.3.2 Tightness of the Lower Bound

Having established that the upper bound to capacity region given by Equations 3.2, 3.3, and 3.4 of Lemma 3 is asymptotically tight, it stands to reason that the lower bound must also be asymptotically tight as well. The lower bound given by Equation 3.12 of Lemma 4 is mainly a function of the crossover probabilities p_0 and p_α. The crossover probabilities are functions of σ_1^2 and σ_2^2, which are functions of μ. Taking

their limits as $\mu \to \infty$:

$$\begin{aligned}
\lim_{\mu\to\infty} \sigma_1^2 &= \lim_{\mu\to\infty} \frac{\varepsilon}{\mu p}\sigma_F^2 + 1 \\
&= 1 \\
\lim_{\mu\to\infty} \sigma_2^2 &= \lim_{\mu\to\infty} 2\frac{\varepsilon}{\mu p}\sigma_F^2 + 1 \\
&= 1 \\
\lim_{\mu\to\infty} p_0 &= \lim_{\mu\to\infty} (1-p)\exp\left(-\beta^2\right) + p\ \exp\left(-\frac{\beta^2}{\sigma_1^2}\right) \\
&= \lim_{\mu\to\infty} (1-p)\exp\left(-\frac{\sigma_2^2}{\sigma_2^2-1}\ln\left[\frac{(1-p)^2\sigma_2^2}{p^2}\right]\right) + \\
&\quad p\ \exp\left(-\frac{\sigma_2^2}{\sigma_1^2(\sigma_2^2-1)}\ln\left[\frac{(1-p)^2\sigma_2^2}{p^2}\right]\right) \\
&= \lim_{\sigma_1^2,\sigma_2^2\to 1} (1-p)\exp\left(-\frac{\sigma_2^2}{\sigma_2^2-1}\ln\left[\frac{(1-p)^2\sigma_2^2}{p^2}\right]\right) + \\
&\quad p\ \exp\left(-\frac{\sigma_2^2}{\sigma_1^2(\sigma_2^2-1)}\ln\left[\frac{(1-p)^2\sigma_2^2}{p^2}\right]\right) \\
&= 0 \\
\lim_{\mu\to\infty} p_\alpha &= \lim_{\mu\to\infty} (1-p)\left(1-\exp\left(-\frac{\beta^2}{\sigma_1^2}\right)\right) + p\ \left(1-\exp\left(-\frac{\beta^2}{\sigma_2^2}\right)\right) \\
&= \lim_{\mu\to\infty} (1-p)\left(1-\exp\left(-\frac{\sigma_2^2}{\sigma_1^2(\sigma_2^2-1)}\ln\left[\frac{(1-p)^2\sigma_2^2}{p^2}\right]\right)\right) + \\
&\quad p\ \left(1-\exp\left(-\frac{1}{\sigma_2^2-1}\ln\left[\frac{(1-p)^2\sigma_2^2}{p^2}\right]\right)\right) \\
&= \lim_{\sigma_1^2,\sigma_2^2\to 1} (1-p)\left(1-\exp\left(-\frac{\sigma_2^2}{\sigma_1^2(\sigma_2^2-1)}\ln\left[\frac{(1-p)^2\sigma_2^2}{p^2}\right]\right)\right) + \\
&\quad p\ \left(1-\exp\left(-\frac{1}{\sigma_2^2-1}\ln\left[\frac{(1-p)^2\sigma_2^2}{p^2}\right]\right)\right) \\
&= 1
\end{aligned}$$

The above steps show that asymptotically, if MAP detection is used, then as $\mu \to \infty$, then the receiver will always decide that a 0 was sent. Furthermore, the probabilities decay towards their limiting value exponentially. Since the lower bound to capacity is $C \geq W\mu f(p_0, p_\alpha)$, the exponential convergence of p_0 and p_α dominates over the linear increase of $W\mu$, the lower bound to capacity decays to zero as $\mu \to \infty$. Therefore, Equations 3.2, 3.3, 3.4 (for the upper bound to capacity region) and 3.12 are tight

bounds to capacity.

3.4 Analysis of Results

Having already examined the behavior of the system in the single user case, it is expected that many of the results obtained in Section 2.4 will also hold for the multiple access scenario. This section will focus on distilling results significant and particular to the multiple access scenario. Where it arises, differences between the multi-access case and the single user case will be noted.

3.4.1 Upper Bound to Multi-access Capacity Region

From information theory the capacity region of a two user multi-access channel is the closure of the convex hull of the set of points (C_1, C_2) satisfying:

$$\begin{aligned} C_1 &\leq I(\underline{X}_1; \underline{Y} | \underline{X}_2) \\ C_2 &\leq I(\underline{X}_2; \underline{Y} | \underline{X}_1) \\ C_1 + C_2 &\leq I((\underline{X}_1, \underline{X}_2); \underline{Y}) \end{aligned}$$

The bounds to the above capacity region were proved in Lemma 3 and given by Equations 3.2, 3.3, and 3.4 respectively. Using some parameters for a common communications channel where $W = 100KHz$, $\sigma_F^2 = 4$, $\gamma = 100$, $T = 0.1$, and $\mathcal{E} = 20$, Figure 3-2 plots the upper bound to capacity regions for several values of μ.

The plots show an interesting phenomenon. Assuming that the users are allowed to transmit at the same rate (i.e., $R_1 = R_2$), the plots indicate that for low values of μ, the maximum rate that the two users can transmit is significantly lower than if there were only one user transmitting. As μ increases, the achievable rate of two users transmitting simultaneously approaches that of the rate achieved by only one user transmitting. One possible way to interpret this result is that for low values of μ, the interference resulting from the presence of the other user (the Multiple Access Interference – MAI), dominates over the interference resulting from the additive re-

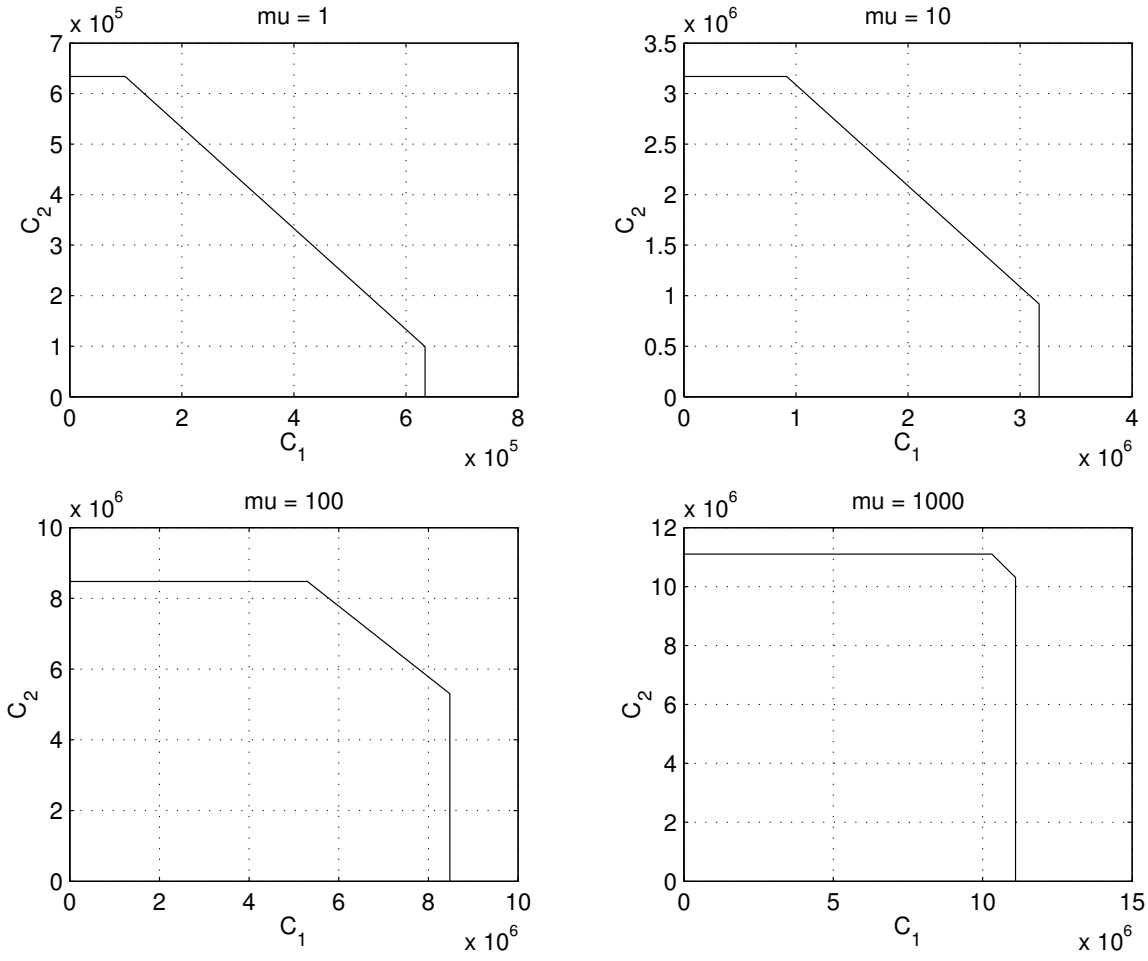

Figure 3-2: Upper Bound to Capacity Region for different μ

ceiver noise. As the μ increases, the effect of MAI mitigates and the achievable rate is mainly hampered by the additive receiver noise. This result agrees with what is expected based on the channel model. With increasing number of coherence bands used for transmission, the power available to each coherence bands decrease. For lower numbers of μ, each user within each coherence band still has enough power that its interference dominates over the additive noise. For large values of μ, the power of each user within each coherence band is so small that the achievable rate is limited by the additive receiver noise.

3.4.2 Comparison of the Upper Bound to Lower Bound

In the multiple access scenario, the upper bound is a capacity region with sets of achievable rates. To make for meaningful comparison with the lower bound, which is just one set of points where each user transmits at the same rate and treats the signal of all other users as noise, use the set of points in the upper bound where each user also transmits with the same rate. In the two user case, the pair of achievable rates in the upper bound where $R_1 = R_2$ corresponds to:

$$R_1 = R_2 = \frac{1}{2} I\left((\underline{X}_1, \underline{X}_2); \underline{Y}\right)$$

where $I(\underline{X}_1, \underline{X}_2; \underline{Y})$ is given by Equation 3.4, making R_1, R_2:

$$R_1 = R_2 = \frac{1}{2}\left\{W\mu \log\left(2\sigma_F^2 \frac{\mathcal{E}}{\mu} + 1\right) - \frac{\mathcal{E}^2}{\gamma^2 T} \log\left(2TW \frac{\gamma}{\sqrt{\mu\mathcal{E}}} \sigma_F^2 + 1\right)\right\}$$

Figure 3-3 shows such an example. For a given $\mu = 100$, the set of rates chosen for comparison are such that $R_1 = R_2$ in both the upper and lower bound. Henceforth, any result that involves application of the upper bound assumes that the above rate is used.

Recall from Section 2.4 that in the single user scenario, decreasing power did not result in capacity gains despite lowering p. However, in the two user scenario, the presence of MAI would suggest that there is a fine balance between the amount of power to use. Using too much power would mean that users suffer from significant MAI. Using less power for each user, while reducing MAI, would also negatively affect the capacity of the user. Plotting the lower bound for several values of $\mathcal{E}$, (using some common parameters $W = 100KHz$, $\sigma_F^2 = 16$, $\gamma = 100$, $T = 0.1$, and $p = \frac{\mathcal{E}^2}{\gamma^2}$) confirms that too much power indeed is detrimental.

The left side of Figure 3-4 shows several plots of the lower bound for different values of $\mathcal{E}$. As is readily evident, for low values of $\mathcal{E}$, increasing $\mathcal{E}$ leads to higher maximum achievable rate. However, comparing the curves for $\mathcal{E} = 50$ and $\mathcal{E} = 80$ shows that use too much power and the achievable rate drops dramatically. Recall

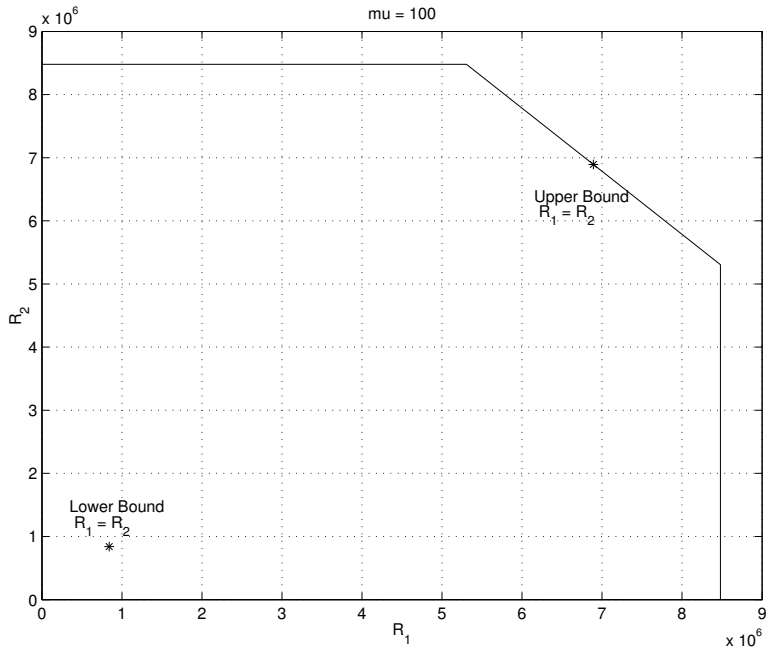

Figure 3-3: Achievable Rates used in Comparison of Upper and Lower Bound

also that it was shown in the single user case that too much power leads to a high p, which significantly reduces the achievable rate. The question that remains then is which of the two factors, MAI or high duty cycle (i.e. high p), is the dominant cause of this drop in achievable rate in the lower bound. Regardless of which is the dominant effect, the end result is the same. Too much power is bad.

The fact that using too much power is bad is reinforced by the right side of Figure 3-4. This plot shows that increasing $\mathcal{E}$ increases the minimum number of coherence bands μ to spread, until $\mathcal{E}$ is between 50 and 60, when the minimum spread factor starts to plummet. Keep in mind however that this result is particular to having chosen binary on-off signaling, which limits $\mathcal{E} \leq \gamma$. Nevertheless, the effect of MAI at high $\mathcal{E}$ cannot be ignored, and the above result indirectly supports the assertion that the transmit power of each user should be limited.

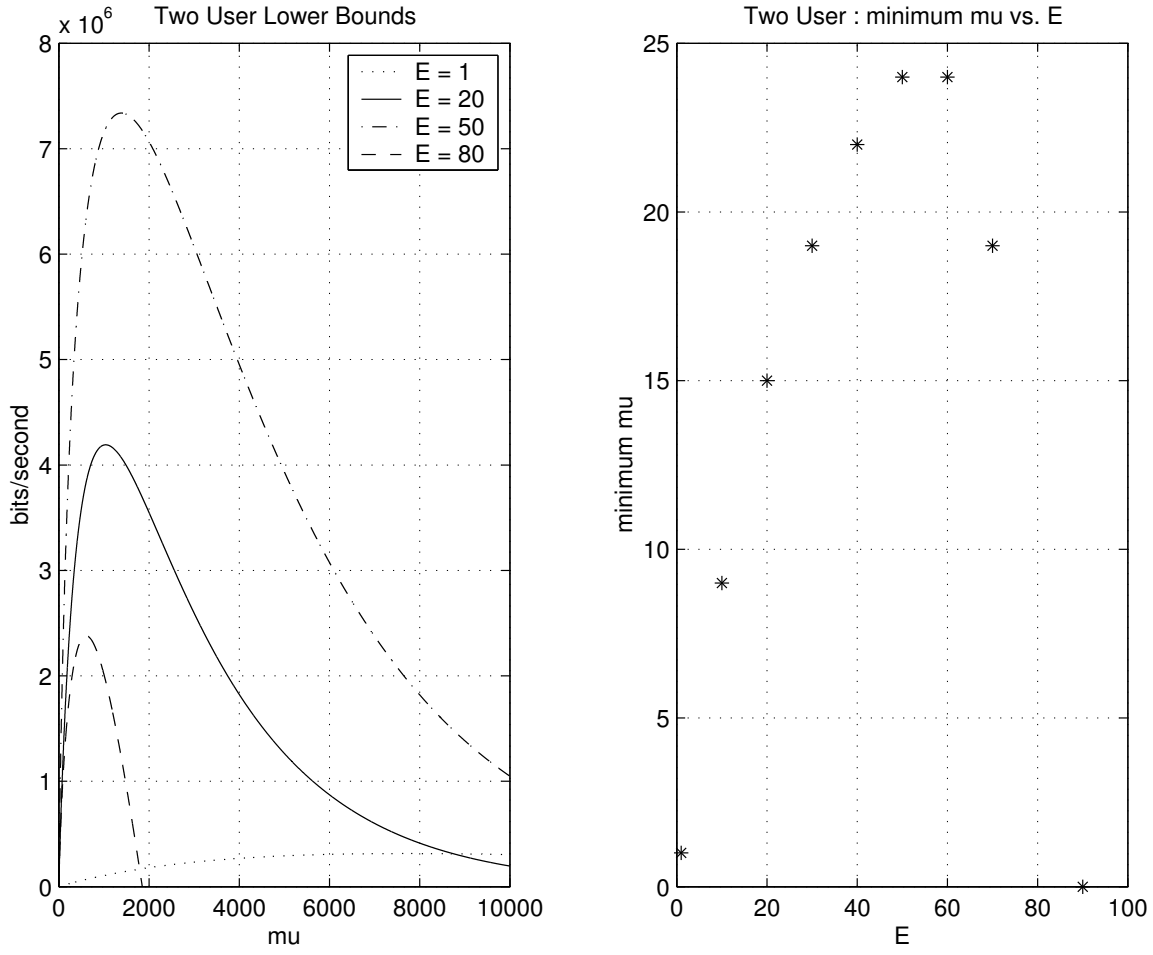

Figure 3-4: Two User: Effect of Varying $\mathcal{E}$

3.4.3 Effect of Varying Parameters

The upper and lower bounds to capacity are functions of the several parameters: W, $\mathcal{E}$, σ_F^2, T, γ, and p. When examining the upper and lower bounds to capacity, these six parameters provide various degrees of freedom that can affect the optimal spreading bandwidth. Many of the results obtained for varying the above parameters in the single user case hold for the two-user case as well. In particular, the significance of σ_F^2 is such that it warrants a second pass here.

The Significance of σ_F^2

$$\beta = \sqrt{\frac{\sigma_2^2}{\sigma_2^2 - 1} \ln \left[\frac{(1-p)^2 \sigma_2^2}{p^2} \right]}$$

The parameter σ_F^2 represents energy of the propagation coefficient, and is particularly significant in the determining the capacity of the lower bound. In the lower bound, because MAP detection is used, σ_F^2 determines detection threshold and therefore determines the crossover probabilities. As can be seen from the equation of the detection threshold β as a function of σ_F^2, repeated above, the greater σ_F^2 is, the easier it is for receiver to figure out which signal $X \in \{0, \alpha\}$ was sent. Therefore, the lower bound to capacity would be expected to increase significantly as σ_F^2 increases. A number of trials were run with some common parameters $W = 100KHz$, $\gamma = 100$, $\mathcal{E} = 20$, $T = 0.1$, and $p = 0.04$ (satisfying the constraint in Equation 2.17 with equality) with varying σ_F^2. The minimum number of coherence bands μ to spread to as σ_F^2 was varied, plotted in Figure 3-5 shows that there is a linear relationship between the energy of the fading coefficient σ_F^2 and minimum μ. However, since the domain of μ is the set of all positive integers, if the plot is made with sufficiently fine granularity, it will show a step-wise change as σ_F^2 is varied. Recall that in the single user case, the staircase behavior was shown in Figure 2-6 of Section 2.4.1.

Also plotted on the same figure is the result from the single user case. As is readily evident, the presence of a second user reduces the minimum spreading bandwidth by a factor of almost two.

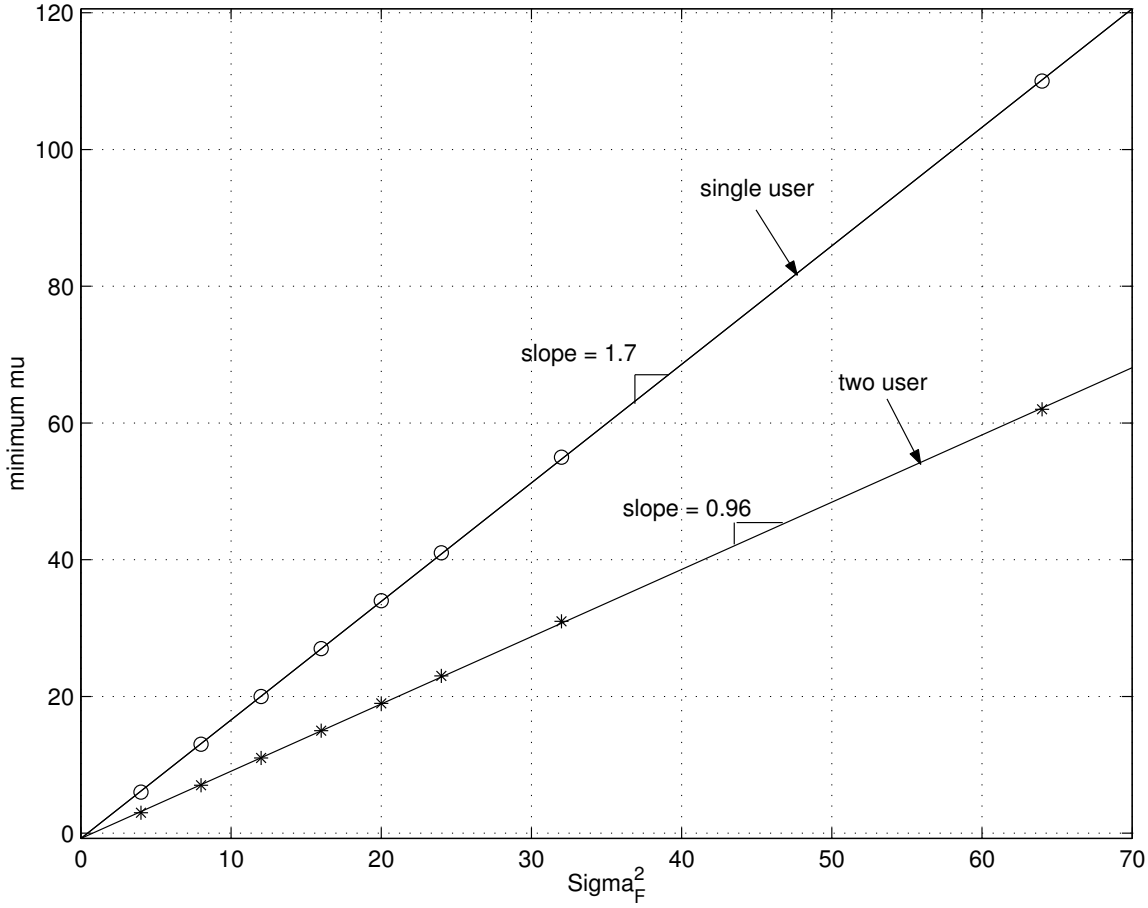

Figure 3-5: σ_F^2 vs. minimum μ

Chapter 4

Conclusion and Further Work

The results the preceding chapters several results of note. Of course, these results are particular to the specific channel model and signaling scheme chosen. Nevertheless, they provide reasonable references for future work. For a DS-CDMA system on time and frequency fading channels, this thesis showed that given an average power constraint and peak signal amplitude constraint, capacity goes to zero as bandwidth increases to infinity. Moreover, by combining the upper bound with a suitable lower bound, the following results were determined:

- taking the energy of the propagation coefficient σ_F^2 as a metric of the signal power, then the minimum number of coherence bands μ to spread is a linear function of the σ_F^2. Furthermore, when extended to the two user scenario, the presence of a second user reduces the minimum spreading bandwidth by a factor of almost two.

- the linear relationship between σ_F^2 and minimum spreading bandwidth is significant in the following sense. For the single user case, given that the relevant parameters are $W = 100\,\text{KHz}$, $\gamma = 100$, $\mathcal{E} = 20$, $T = 0.1\,\text{sec}$, and $p = 0.04$, for $\sigma_F^2 = 8$, the minimum number of coherence bands to spread is $\mu = 13$. Since each coherence bandwidth is of size $W = 100\,\text{KHz}$, that means given the system parameters, the system should be spread to 1.3 MHz. Considering that the commercial DS-CDMA system IS-95 transmits at a bandwidth of 1.25 MHz,

these results serve as meaningful references for designing future communication systems.

Despite having obtained some meaningful results, further work remains to be done. In particular, the possibility of a tighter lower bound that is not dependent on any specific signaling scheme should be explored. Expanding the two user multiple access scenario to the general N user case may also be explored.

Appendix A

Equations and Proofs

Lemma 5 *Let $\underline{Z}_n$ be a zero mean, complex circularly symmetric Gaussian random vector with covariance matrix $\Lambda_{\underline{Z}_n}$, its PDF is:*

$$f_{\underline{Z}_n}(\underline{z}_n) = \frac{1}{(\pi)^n |\Lambda_{\underline{Z}_n}|} \exp\left\{-\underline{Z}_n^H \Lambda_{\underline{Z}_n}^{-1} \underline{Z}_n\right\} \tag{A.1}$$

Proof:

Since each circularly symmetric complex Gaussian random variable can be expressed as a random vector of two independent, identically distributed Gaussian random variables $\underline{Z}_n$ can be expressed as two independent, identically distributed Gaussian random vectors:

$$\underline{Z}_n = \underline{Y}_{2n} = \begin{bmatrix} \underline{Z}_{Rn} \\ \underline{Z}_{In} \end{bmatrix}$$

and the covariance of matrix of $\underline{Y}_{2n}$ can be expressed as:

$$\begin{aligned} \Lambda_{\underline{Y}_{2n}} &= \begin{bmatrix} \Lambda_{\underline{Z}_{Rn}} & 0 \\ 0 & \Lambda_{\underline{Z}_{In}} \end{bmatrix} \\ |\Lambda_{\underline{Y}_{2n}}| &= |\Lambda_{\underline{Z}_{Rn}}||\Lambda_{\underline{Z}_{In}}| \end{aligned}$$

now, because of circular symmetry, $\Lambda_{\underline{Z}_{Rn}} = \Lambda_{\underline{Z}_{In}} = \frac{1}{2}\Lambda_{\underline{Z}_n}$

$$\begin{aligned}
f_{\underline{Z}_n}(\underline{z}_n) &= f_{\underline{Y}_{2n}}(\underline{y}_{2n}) = f_{\underline{Z}_{Rn}}(\underline{z}_{Rn}) f_{\underline{Z}_{In}}(\underline{z}_{In}) \\
&= \frac{1}{\sqrt{(2\pi)^n |\Lambda_{\underline{Z}_{Rn}}|}} \exp\left\{-\frac{1}{2}(\underline{Z}_{Rn}^T \Lambda_{\underline{Z}_{Rn}}^{-1} \underline{Z}_{Rn})\right\} \times \\
&\quad \frac{1}{\sqrt{(2\pi)^n |\Lambda_{\underline{Z}_{In}}|}} \exp\left\{-\frac{1}{2}(\underline{Z}_{In}^T \Lambda_{\underline{Z}_{In}}^{-1} \underline{Z}_{In})\right\} \\
&= \frac{1}{(2\pi)^n |\Lambda_{\underline{Z}_{Rn}}|^{1/2} |\Lambda_{\underline{Z}_{In}}|^{1/2}} \exp\left\{-\frac{1}{2}(\underline{Z}_{Rn}^T \Lambda_{\underline{Z}_{Rn}}^{-1} \underline{Z}_{Rn} + \underline{Z}_{In}^T \Lambda_{\underline{Z}_{In}}^{-1} \underline{Z}_{In})\right\} \\
&= \frac{1}{(2\pi)^n |\frac{1}{2}\Lambda_{\underline{Z}_n}|^{1/2} |\frac{1}{2}\Lambda_{\underline{Z}_{Rn}}|^{1/2}} \exp\left\{-\frac{1}{2}\left[\underline{Z}_n^T (\frac{1}{2}\Lambda_{\underline{Z}_n})^{-1} \underline{Z}_{Rn} + \underline{Z}_{In}^T (\frac{1}{2}\Lambda_{\underline{Z}_n})^{-1} \underline{Z}_{In}\right]\right\} \\
&= \frac{1}{(2\pi)^n |\frac{1}{2}\Lambda_{\underline{Z}_n}|} \exp\left\{-\left[\underline{Z}_{Rn}^T \Lambda_{\underline{Z}_n}^{-1} \underline{Z}_{Rn} + \underline{Z}_{In}^T \Lambda_{\underline{Z}_n}^{-1} \underline{Z}_{In}\right]\right\} \\
&= \frac{1}{(\pi)^n |\Lambda_{\underline{Z}_n}|} \exp\left\{-\underline{Z}_n^H \Lambda_{\underline{Z}_n}^{-1} \underline{Z}_n\right\} \qquad \textbf{\textit{Q.E.D.}}
\end{aligned}$$

Lemma 6 *Let $\underline{Z}_n$ be a zero mean, complex circularly symmetric Gaussian random vector with covariance matrix $\Lambda_{\underline{Z}_n}$, its entropy is:*

$$h\left(\underline{Z}_n\right) = \log\left(\pi e\right)^n |\Lambda_{\underline{Z}_n}| \tag{A.2}$$

Proof:

From Lemma 5, the probability density function of $\underline{Z}_n$ is:

$$f_{\underline{Z}_n}\left(\underline{z}_n\right) = \frac{1}{\pi^n |\Lambda_{\underline{Z}_n}|} \exp\{-\underline{Z}_n^H \Lambda_{\underline{Z}_n}^{-1} \underline{Z}_n\}$$

Then from the definition of differential entropy:

$$\begin{aligned}
h(\underline{Z}_n) &= E\left[-\ln f_{\underline{Z}_n}(\underline{z}_n)\right] \\
&= -\int f_{\underline{Z}_n}(\underline{z}_n) \times \ln\left[\frac{1}{(\pi)^n |\Lambda_{\underline{Z}_n}|} \exp\{-\underline{Z}_n^H \Lambda_{\underline{Z}_n}^{-1} \underline{Z}_n\}\right] \, d\underline{z}_n \\
&= \ln(\pi^n |\Lambda_{\underline{Z}_n}|) + \int f_{\underline{Z}_n}(\underline{z}_n) \left[\underline{Z}_n^H \Lambda_{\underline{Z}_n}^{-1} \underline{Z}_n\right] \, d\underline{z}_n \\
&= \ln(\pi^n |\Lambda_{\underline{Z}_n}|) + E\left[\underline{Z}_n^H \Lambda_{\underline{Z}_n}^{-1} \underline{Z}_n\right]
\end{aligned}$$

$$
\begin{aligned}
&= \ln(\pi^n|\Lambda_{\underline{Z}_n}|) + E\left[\sum_{i,j} z_i^*(\Lambda^{-1})_{ij} z_j\right] \\
&= \ln(\pi^n|\Lambda_{\underline{Z}_n}|) + E\left[\sum_{i,j} z_i^* z_j(\Lambda^{-1})_{ij}\right] \\
&= \ln(\pi^n|\Lambda_{\underline{Z}_n}|) + \sum_{i,j} E\left[z_i^* z_j\right](\Lambda^{-1})_{ij} \\
&= \ln(\pi^n|\Lambda_{\underline{Z}_n}|) + \sum_{i}\sum_{j} \Lambda_{ji}(\Lambda^{-1})_{ij} \\
&= \ln(\pi^n|\Lambda_{\underline{Z}_n}|) + \sum_{j} I_{jj} \\
&= \ln(\pi^n|\Lambda_{\underline{Z}_n}|) + n \\
&= \ln e^n + \ln(\pi^n|\Lambda_{\underline{Z}_n}|) \\
&= \ln\left[(\pi e)^n|\Lambda_{\underline{Z}_n}|\right] \text{ nats} \\
&= \log(\pi e)^n|\Lambda_{\underline{Z}_n}| \text{ bits} \qquad \textbf{\textit{Q.E.D.}}
\end{aligned}
$$

Lemma 7 *Let the covariance matrix of $\underline{Y}_n$ given $\underline{X}_n$ be given as follows:*

$$
\Lambda_{\underline{Y}_n|\underline{X}_n} = \begin{bmatrix}
\sigma_F^2 x[1]^2 + 1 & \sigma_F^2 x[1]x[2] & \cdots & \sigma_F^2 x[1]x[n] \\
\sigma_F^2 x[2]x[1] & \sigma_F^2 x[2]^2 + 1 & \cdots & \sigma_F^2 x[2]x[n] \\
\vdots & \vdots & \ddots & \vdots \\
\sigma_F^2 x[n]x[1] & \sigma_F^2 x[n]x[2] & \cdots & \sigma_F^2 x[n]^2 + 1
\end{bmatrix} \tag{A.3}
$$

then the eigenvalues of $\Lambda_{\underline{Y}_n|\underline{X}_n}$ are:

$$
\begin{aligned}
\lambda_j &= 1 && \text{for } j = 1 \ldots n-1 \\
\lambda_j &= \sigma_F^2 \|\underline{x}_n\|^2 + 1 && \text{for } j = n
\end{aligned} \tag{A.4}
$$

Proof:

$\Lambda_{\underline{Y}_n|\underline{X}_n} = \sigma_F^2 \tilde{\Lambda}_n + I_n$ where I_n is the identity matrix and $\tilde{\Lambda}_n$ is as follows:

$$
\tilde{\Lambda}_n = \begin{bmatrix}
x[1]^2 & x[1]x[2] & \cdots & x[1]x[n] \\
x[2]x[1] & x[2]^2 & \cdots & x[2]x[n] \\
\vdots & \vdots & \ddots & \vdots \\
x[n]x[1] & x[n]x[2] & \cdots & x[n]^2
\end{bmatrix}
$$

the problem of calculating λ_i, the eigenvalues of $\Lambda_{\underline{Y}_n|\underline{X}_n}$, therefore reduces down to finding $\tilde{\lambda}_i$, the eigenvalues of $\tilde{\Lambda}_n$. Where $\lambda_i = \sigma_F^2 \tilde{\lambda}_i + 1$.

Now show that $\tilde{\lambda} = \|x_n\|^2$ is an eigenvalue of $\tilde{\Lambda}_n$ by finding the corresponding eigenvector $\underline{W}_n$.

From the definition of eigenvalue – eigenvector pair:

$$\begin{bmatrix} x[1]^2 & x[1]x[2] & \cdots & x[1]x[n] \\ x[2]x[1] & x[2]^2 & \cdots & x[2]x[n] \\ \vdots & \vdots & \ddots & \vdots \\ x[n]x[1] & x[n]x[2] & \cdots & x[n]^2 \end{bmatrix} \begin{bmatrix} w[1] \\ w[2] \\ \vdots \\ w[n] \end{bmatrix} = \|\underline{x}\|^2 \begin{bmatrix} w[1] \\ w[2] \\ \vdots \\ w[n] \end{bmatrix} \tag{A.5}$$

Now expand the matrix equation A.5 into a system of n linear equations, and constraining $\|\underline{w}_n\|^2 = 1$.

$$\begin{aligned} x[1]\sum_i x[i]w[i] &= w[1]\sum_i x[i]^2 \\ x[2]\sum_i x[i]w[i] &= w[2]\sum_i x[i]^2 \\ &\vdots \\ x[n]\sum_i x[i]w[i] &= w[n]\sum_i x[i]^2 \end{aligned}$$

Taking the ratio of any two of the above system of linear equations yields:

$$\begin{aligned} \tfrac{x[k]}{x[l]} &= \tfrac{w[k]}{w[l]} \quad \text{for } k,l \in \{1,2,\ldots n\} \\ w_k &= w_l \tfrac{x_k}{x_l} \quad \text{for } k,l \in \{1,2,\ldots n\} \end{aligned}$$

Express $w[k],\ k \neq n$ in terms of $w[n]$ and $x[l],\ l \in \{1,2,\ldots n\}$, to solve for $w[n]$.

$$\begin{aligned} w[1] &= w[n]\tfrac{x[1]}{x[n]} \quad \Rightarrow \quad w[1]^2 = w[n]^2\tfrac{x[1]^2}{x[n]^2} \\ w[2] &= w[n]\tfrac{x[2]}{x[n]} \quad \Rightarrow \quad w[2]^2 = w[n]^2\tfrac{x[2]^2}{x[n]^2} \\ &\vdots \\ w[n-1] &= w[n]\tfrac{x[n-1]}{x[n]} \quad \Rightarrow \quad w[n-1]^2 = w[n]^2\tfrac{x[n-1]^2}{x[n]^2} \end{aligned}$$

$$
\begin{aligned}
w[1]^2 + w[2]^2 + \cdots + w[n-1]^2 &= w[n]^2 \left(\tfrac{x[1]^2+x[2]^2+\cdots+x[n-1]^2}{x[n]^2}\right) \\
\underbrace{w[1]^2 + w[2]^2 + \cdots + w[n-1]^2 + w[n]^2}_{\|\underline{w}_n\|^2=1} &= w[n]^2 \left(\tfrac{x[1]^2+x[2]^2+\cdots+x[n-1]^2}{x[n]^2}\right) + w[n]^2 \\
1 &= w[n]^2 \left(\tfrac{x[1]^2+x[2]^2+\cdots+x[n-1]^2}{x[n]^2} + \tfrac{x[n]^2}{x[n]^2}\right) \\
1 &= w[n]^2 \left(\tfrac{\|\underline{x}_n\|^2}{x[n]^2}\right) \\
w[n]^2 &= \tfrac{x_n^2}{\|\underline{x}_n\|^2} \\
w[n] &= \tfrac{x[n]}{\|\underline{x}_n\|}
\end{aligned}
\tag{A.6}
$$

Extending the result derived in Equation A.6, conclude that $\tilde{\lambda} = \|x_n\|^2$ is an eigenvalue of $\tilde{\Lambda}_n$ with eigenvector $\underline{W}_n = \left[\frac{x[1]}{\|x_n\|}, \frac{x[2]}{\|x_n\|}, \ldots, \frac{x[n]}{\|x_n\|}\right]^T$

From linear algebra and the properties of covariance matrices, the following are known:

- covariance matrices are positive semidefinite $\rightarrow$ all eigenvalues are non-negative.
- $trace(\tilde{\Lambda}_n) = \|x_n\|^2 = \sum_i \tilde{\lambda}_i$
- since Equation A.6 showed that $\|x_n\|^2$ is an eigenvalue of $\tilde{\Lambda}$, which equal to $trace(\tilde{\Lambda}_n) = \sum_i \tilde{\lambda}_i$, all the other eigenvalues must be zero.

Given that $\lambda_i = \sigma_F^2 \tilde{\lambda}_i + 1$, conclude:

$$
\begin{aligned}
\tilde{\lambda_j} &= 0 \quad \Rightarrow \quad \lambda_j = 1 && \text{for } j = 1 \ldots n-1 \\
\tilde{\lambda_j} &= \|\underline{x}_n\|^2 \quad \Rightarrow \quad \lambda_j = \sigma_F^2 \|\underline{x}_n\|^2 + 1 && \text{for } j = n
\end{aligned}
$$

Q.E.D.

Lemma 8 *Let the covariance matrix of $\underline{Y}_n$ given $\underline{X}_{1,n}$ and $\underline{X}_{2,n}$ be given as follows:*

$$
\Lambda_{\underline{Y}_n|\underline{X}_{1,n}\underline{X}_{2,n}} = \begin{bmatrix}
\sigma_F^2\left(x_1[1]^2 + x_2[1]^2\right) + 1 & \sigma_F^2\left(x_1[1]x_1[2] + x_2[1]x_2[2]\right) & \cdots & \sigma_F^2\left(x_1[1]x_1[n] + x_1[1]x_1[n]\right) \\
\sigma_F^2\left(x_1[2]x_1[1] + x_2[2]x_2[1]\right) & \sigma_F^2\left(x_1[2]^2 + x_2[2]^2\right) + 1 & \cdots & \sigma_F^2\left(x_1[2]x_1[n] + x_2[2]x_2[n]\right) \\
\vdots & \vdots & \ddots & \vdots \\
\sigma_F^2\left(x_1[n]x_1[1] + x_2[n]x_2[1]\right) & \sigma_F^2\left(x_1[n]x_1[2] + x_2[n]x_2[2]\right) & \cdots & \sigma_F^2\left(x_1[n]^2 + x_2[n]^2\right) + 1
\end{bmatrix}
\tag{A.7}
$$

then the eigenvalues of $\Lambda_{\underline{Y}_n|\underline{X}_n}$ *are:*

$$\begin{aligned}
\lambda_j &= 1 && \text{for } j = 1 \ldots n-2 \\
\lambda_j &= \tfrac{\sigma_F^2}{2}\left(\|\underline{x}_{1,n}\|^2 + \|\underline{x}_{2,n}\|^2\right) \\
&\quad + \tfrac{\sigma_F^2}{2}\left(\sqrt{\left[\|\underline{x}_{1,n}\|^2 + \|\underline{x}_{2,n}\|^2\right]^2 - 4\sum_{k=1}^{TW-1}\sum_{l=k+1}^{TW}(x_1[k]x_2[l] - x_1[l]x_2[k])^2}\right) + 1 && \text{for } j = n-1 \\
\lambda_j &= \tfrac{\sigma_F^2}{2}\left(\|\underline{x}_{1,n}\|^2 + \|\underline{x}_{2,n}\|^2\right) \\
&\quad - \tfrac{\sigma_F^2}{2}\left(\sqrt{\left[\|\underline{x}_{1,n}\|^2 + \|\underline{x}_{2,n}\|^2\right]^2 - 4\sum_{k=1}^{TW-1}\sum_{l=k+1}^{TW}(x_1[k]x_2[l] - x_1[l]x_2[k])^2}\right) + 1 && \text{for } j = n
\end{aligned} \tag{A.8}$$

Proof:

$\Lambda_{\underline{Y}_n|\underline{X}_{1,n},\underline{X}_{2,n}} = \sigma_F^2\tilde{\Lambda}_n + I_n$ where I_n is the identity matrix and $\tilde{\Lambda}_n$ is as follows:

$$\tilde{\Lambda}_n = \begin{bmatrix}
x_1[1]^2 + x_2[1]^2 & x_1[1]x_1[2] + x_2[1]x_2[2] & \cdots & x_1[1]x_1[n] + x_2[1]x_2[n] \\
x_1[2]x_1[1] + x_2[2]x_2[1] & x_1[2]^2 + x_2[2]^2 & \cdots & x_1[2]x_1[n] + x_2[2]x_2[n] \\
\vdots & \vdots & \ddots & \vdots \\
x_1[n]x_1[1] + x_2[n]x_2[1] & x_1[n]x_1[2] + x_2[n]x_2[2] & \cdots & x_1[n]^2 + x_2[n]^2
\end{bmatrix}$$

the problem of calculating λ_i, the eigenvalues of $\Lambda_{\underline{Y}_n|\underline{X}_n}$, therefore reduces down to finding $\tilde{\lambda}_i$, the eigenvalues of $\tilde{\Lambda}_n$. Where $\lambda_i = \sigma_F^2\tilde{\lambda}_i + 1$.

The eigenvalues of $\tilde{\Lambda}_n$ can be calculated by solving the following:

$$|\tilde{\Lambda}_n - \lambda I_n| = 0$$

which yields the following eigenvalues:

$$\begin{aligned}
\lambda_j &= 0 && \text{for } j = 1 \ldots n-2 \\
\lambda_j &= \tfrac{1}{2}\left(\|\underline{x}_{1,n}\|^2 + \|\underline{x}_{2,n}\|^2\right) \\
&\quad + \tfrac{1}{2}\left(\sqrt{\left[\|\underline{x}_{1,n}\|^2 + \|\underline{x}_{2,n}\|^2\right]^2 - 4\sum_{k=1}^{TW-1}\sum_{l=k+1}^{TW}(x_1[k]x_2[l] - x_1[l]x_2[k])^2}\right) && \text{for } j = n-1 \\
\lambda_j &= \tfrac{1}{2}\left(\|\underline{x}_{1,n}\|^2 + \|\underline{x}_{2,n}\|^2\right) \\
&\quad - \tfrac{1}{2}\left(\sqrt{\left[\|\underline{x}_{1,n}\|^2 + \|\underline{x}_{2,n}\|^2\right]^2 - 4\sum_{k=1}^{TW-1}\sum_{l=k+1}^{TW}(x_1[k]x_2[l] - x_1[l]x_2[k])^2}\right) && \text{for } j = n
\end{aligned}$$

Given that $\lambda_i = \sigma_F^2\tilde{\lambda}_i + 1$, the eigenvalues of Equation A.8 follow. ***Q.E.D.***

Bibliography

[1] I.C. Abou Faycal, M.D. Trott, and S. Shamai, "The Capacity of Discrete-Time Memoryless Rayleigh Fading Channels," *IEEE Transactions on Information Theory*, Vol. 47, No. 4, May 2001.

[2] R. Ahlswede, "Multi-way Communication Channels," *Proceedings of 2nd International Symposium on Information Theory (Tsahkadsor, Armenian S.S.R.)*, pp. 23-52, Prague, 1971.

[3] T.M. Cover and J.A. Thomas, *Elements of Information Theory*, Wiley Series in Telecommunications, Wiley, New York, 1991.

[4] R.G. Gallager, *Information Theory and Reliable Communications*, John Wiley & Sons, 1968.

[5] R.G. Gallager, M. Médard, "Bandwidth Scaling for Fading Channels", *Proceedings of IEEE International Symposium on Information Theory*, 1997.

[6] B. Hajek, V.G. Subramanian, "Capacity and Reliability Function for Small Peak Signal Constraints," *IEEE Transactions on Information Theory*, Vol. 48, No. 4, April, 2002.

[7] R.S. Kennedy, *Fading Dispersive Communication Channels*, New York: Wiley-Interscience, 1969.

[8] H. Liao, *Multiple Access Channels*, Ph.D. Thesis, University of Hawaii, 1972.

[9] T.L. Marzetta, B.M. Hochwald, "Capacity of a Mobile Multiple-Antenna Communication Link in Rayleigh Flat Fading", *IEEE Transactions on Information Theory*, vol. 45, no. 1, January 1999.

[10] M. Médard, *The Capacity of Time Varying Multiple User Channels in Wireless Communications*, Sc.D. Thesis, MIT, September 1995.

[11] M. Médard, "Bound on Mutual Information for DS-CDMA Spreading over Independent Fading Channels", proceedings of *Asilomar Conference on Signal, Systems and Computers*, November 1997, pp. 187-191.

[12] M. Médard, D.N.C. Tse, "Spreading in Block-Fading Channels", Conference Record of the 34th *Asilomar Conference on Signal, Systems and Computers*, 2000, vol. 2, pp. 1598-1602.

[13] M. Médard, R.G. Gallager, "Bandwidth Scaling for Fading Multipath Channels", *IEEE Transactions on Information Theory*, Vol. 48, No. 4, April, 2002.

[14] V.G. Subramanian, B. Hajek, "Broad-Band Fading Channels: Signal Burstiness and Capacity," *IEEE Transactions on Information Theory*, Vol. 48, No. 4, April, 2002.

[15] E. Telatar, D.N.C. Tse, "Capacity and Mutual Information of Wideband Multipath Fading Channels", *IEEE Transactions on Information Theory*, Vol. 46, No. 4, July 2000.

[16] E. Telatar, *Coding and Multiaccess for the Energy Limited Rayleigh Fading Channel*, S.M. Thesis, MIT, May 1988.